WATKINS, KEITH EDGAR, M.A. Examining Longleaf Pine Spectral Properties to Remotely Map Relict Stands in Central North Carolina. (2017)
Directed by Dr. Paul A. Knapp 51 pp.

This thesis has been prepared as a manuscript for submission and potential publication in a peer-reviewed academic journal. This thesis investigates the unique spectral reflectance properties of 109 "montane" longleaf pine canopies (*Pinus palustris* Mill.) growing on steep, south-facing slopes as well as 51 "piedmont" individuals growing in an area of low topographic relief, all found within the Uwharrie National Forest in central North Carolina. The geographic location of all sampled longleaf canopies were recorded on a digital map, and then spectrally analyzed to derive unique reflectance signatures that would allow for the remote mapping of the species using high-resolution multispectral WorldView-2 satellite imagery. Overall accuracies for classification procedures range from 91–96% between four study sites. Longleaf pine spectral properties were statistically investigated to quantify differences in reflectance due to topography and canopy height. Significant relationships ($p < 0.05$) were found for each variable, and suggest that spectral reflectance values for longleaf pine are not uniform throughout the study area and can vary according to topographic and morphological canopy features.

EXAMINING LONGLEAF PINE SPECTRAL PROPERTIES TO REMOTELY MAP RELICT STANDS IN CENTRAL NORTH CAROLINA

by

Keith Edgar Watkins

A Thesis Submitted to
the Faculty of The Graduate School at
The University of North Carolina at Greensboro
in Partial Fulfillment
of the Requirements for the Degree
Master of Arts

Greensboro
2017

Approved by

_____
Committee Chair

APPROVAL PAGE

This thesis written by Keith Edgar Watkins has been approved by the following committee of the Faculty of The Graduate School at The University of North Carolina at Greensboro.

Committee Chair _____
Paul A. Knapp

Committee Members _____
Roy S. Stine

_____
P. Dan Royall

_____
Date of Acceptance by Committee

_____
Date of Final Oral Examination

ACKNOWLEDGMENTS

I would like to thank my friends, colleagues and professors who have inspired, guided and helped me to cultivate the research that is contained within this thesis. Without the expert guidance of my committee chair, Dr. Paul Knapp, and committee members Dr. Roy Stine and Dr. Dan Royall, this research would not have been possible.

This research required hours of field work to locate individual longleaf samples, and luckily most of it was not spent without the company of Dr. Paul Knapp and Dr. Tommy Patterson at my side, offering encouragement and helping to develop the intricacies of my research. Finally, I would like to thank my wife Kelly, for providing my sanctuary after endless hours spent working in the labs, and for helping me to never give up hope.

This thesis was funded in part by a research travel grant provided by the University of North Carolina at Greensboro's Graduate Student Association, and by the Digital Globe Foundation who has provided the WorldView-2 satellite imagery for this research.

TABLE OF CONTENTS

Page

LIST OF TABLES

Page

LIST OF FIGURES

Page

CHAPTER I

INTRODUCTION

1.1 Historical Background on Longleaf Pine

The longleaf pine ecosystem (Figure 1.1) spanned ~ 37 million hectares within the southern United States prior to European settlement (Jose et al. 2006). Logging and turpentine gathering since the early 1700s, coupled with fire suppression practices beginning in the early 1900s, has diminished the species range to ~4.5% of the original land area with about 25% of this area represented by >25 year-old plantations (Oswalt et al., 2012). The reduction of longleaf pine habitats has provoked researchers and government agencies to initiate protocols to maintain the remaining stands across the southeastern United States (Brockway 2005). Longleaf pine is a keystone species and integral to the success of many organisms, and the ecosystems within which they grow provide habitats for several endangered species including the red-cockaded woodpecker (RWC) (James et al. 2001). The RWC (*Leuconotopicus borealis* Vieillot) was placed on the endangered species list in 1979 with only 10,000 known individuals. RCWs create and inhabit crevices in old-growth pines, where heart rot allows them to create nests. Due to the reduction in old-growth (>150 years old) longleaf pine stands, available habitats are a limiting factor for the species and has been associated with their decline during the 20th century (Carney 2009).

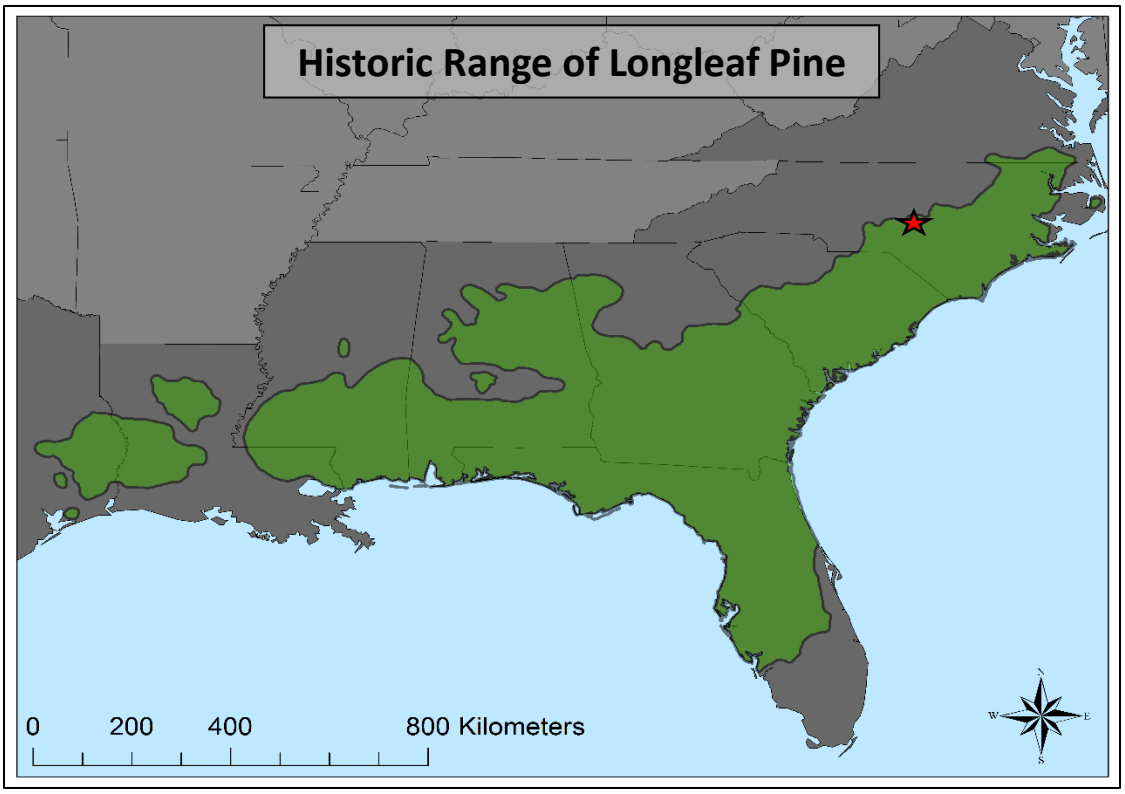

Figure 1.1. The Historic Range Of Longleaf Pine In The Southern United States. Location of Uwharrie National Forest Is Shown As Red Star In Central North Carolina. Source: Arcmap.

Many longleaf pine forests in the North Carolina Piedmont region have been replanted with other pine species such as shortleaf and loblolly as longleaf pine is comparatively slow to germinate and requires frequent (3–5 years) low-intensity fire to be competitive with other species. Combined, these characteristics decrease its economic viability (Jose et al. 2006), which have further reduced its geographic range. Resultantly, there are few intact longleaf pine stands remaining–particularly in the central Piedmont area of North Carolina –and thus few "blueprints" of intact longleaf pine systems exist to improve our understanding of the species.

Most information relating to longleaf systems comes from the sandhills and coastal plain ecoregions, while studies investigating stands growing in "mountain" or "montane" environments are comparatively underrepresented in the literature (Cipollini et al. 2012). The paucity of research relating to these montane longleaf pine communities is troubling, as this longleaf forest type is the most imperiled, inhabiting only two percent of the remnant land area (Edelgard et al. 2000). Further investigation of montane longleaf ecosystems is essential for developing and implementing habitat restoration methods such as prescribed burnings and undergrowth clearing.

Montane communities of longleaf pine are typically found in mountainous areas of northern Alabama and Georgia, and are situated on steep southerly and southwestern slopes within areas of prominent topographic relief (up to 600 m) (Peet 2006, Stokes et al. 2010). Longleaf in montane environments are adapted to shallow, rocky soils, can experience ice and snow at higher elevations, and represent a "physiographically and climactically distinct" region within the natural range of this species (Stokes et al. 2010). This study uses a montane-class distinction of longleaf for samples gathered in areas of high topographic relief (>100 m), and a piedmont-class distinction for samples located in areas with low topographic relief (<20 m).

A forest inventory completed by Patterson and Knapp (2016a) located the only known old-growth montane longleaf pine stands in central North Carolina. Their research, completed in Uwharrie National Forest, noted the rarity of the montane variant, the need to preserve the extant stands by re-establishing frequent low-intensity fires, and the importance of locating other montane stands allowing for further insight into their

optimum reproductive parameters. In short, successful reestablishment of montane stands will be improved if a larger number of stands can be assessed to use as a "blueprint" for site characteristics.

Traditional means of locating tree stands of a specific species often requires extensive surveys to be completed in areas with difficult and hazardous topography such as the Uwharrie Mountains. Spatial and spectral improvements in remote-sensing technology have provided more efficient and precise means for investigating and classifying land cover, and improved vegetation mapping accuracies reduce the necessity of exhaustive field surveys, which are often more costly and cannot provide complete investigation of large areas (Martin et al. 1998). This study investigates the viability of using remote sensing data to aid in the location of remnant longleaf pine stands within the Uwharrie National Forest (UNF), in hopes that they may be mapped and studied to promote the recovery of these rare habitats.

1.2 Background on Remote Vegetation Mapping

Many studies have investigated methodologies for locating individual tree species through the spectral analysis of remotely sensed imagery, allowing for species mapping across wider geographic areas than can be obtained through in-situ investigations (Carter et al. 1998; Di Vittorio & Biging, 2009; Holmgren et al., 2008; Manjunath et al., 2013). This paper intends to add to the growing body of literature on remote-vegetation mapping, while focusing on a specific species of interest: longleaf pine (*Pinus palustris),* growing within the Uwharrie National Forest and surrounding land holdings in central North Carolina.

Traditionally, satellite imagery such as that gathered by the Earth Resources Technology Satellite 1 (ERTS-1), later renamed Landsat-1, provided images with a spatial resolution of 80 m pixels, which is the size of a cell in a derived raster image (Dowman et al. 2014) with electromagnetic wave collection across four spectral bands between 475 to 1100 nm (Jensen, 2007). When Landsat-1 was launched in 1972, the 80 m pixels were used as the basic unit of analysis for the remote sensing of landscapes. Although this imagery provided valuable information relating to the Earth's surface, the inability of the sensor to capture ground objects smaller than that of the pixel size, limited the abilities of the remote-sensing analyst. Smaller objects such as individual tree canopies and houses could not be closely analyzed until sensor technology increased and the spatial resolution provided smaller units of analysis (Blaschke et al. 2008).

The advent of more advanced satellite sensors provided much finer spatial resolution, with modern sensors capable of producing imagery with pixel sizes < 0.5 m (Dowman et al. 2014). In addition to increased spatial resolution, the ability of sensors to gather spectral data across larger portions of the electromagnetic spectrum (EMS) (i.e., ultraviolet and near-infrared (NIR) wavelengths) with greater numbers of discrete bands, allowed for more precise measurements of spectral reflectance within the imagery. These advances have permitted more accurate mapping of vegetation content and health at both small and large scales across the landscape through the analysis of spectral reflectance across different portions of the electromagnetic spectrum (Martin et al. 1998, Coops et al. 2006, Nieminen et al. 2014, Waser et al. 2014).

1.3 Spectral Reflectance Properties of Vegetation

The spectral reflectance characteristics of vegetation are directly related to varying levels of incident light being absorbed, transmitted, scattered and reflected by the plant and its leaves (Richardson et al. 2001). Properties of absorption, transmittance and reflection are influenced both by the surface characteristics of a plant's leaves (size, shape, albedo), and also by the internal structure and biochemical composition within the plant's leaves (Richardson et al. 2001). Different types of vegetation contain varying concentrations of chlorophyll and pigments, causing variations in reflectance across the visible and NIR portions of the spectrum for different species (Carter 1993). Analysis of spectral reflectance gathered from multispectral sensors can reveal distinguishing reflectance characteristics related to plant stress (Waser et al. 2014), variations between tree species (van Aardt and Wynne 2001), and leaf age (Carter et al. 1989). Measurements of these spectral variations allow an analyst to identify unique spectral signatures within the imagery that pertain to either specific species or varying levels of plant health. Successful spectral discrimination of reflectance values pertaining to individual tree types in digital imagery can allow for species mapping across large geographic areas.

External factors can also influence the measured spectral reflectance of tree canopies, including variations in incoming solar radiation due to elevation, slope and aspect, tree height, stand openness (Carter et al. 1989), and tree-health variations associated with topography (Richardson et al. 2001). Trees growing along elevational gradients can decrease photosynthetic efficiency with height, limiting their potential to

endure environmental stressors (Richardson et al. 2001). For certain species, changes in environmental conditions relating to higher elevation can lead to adaptation mechanisms such as producing foliage with waxy cuticles, low surface area as well as lignified tissue (Richardson et al. 2002). Physiological adaptations in plants, especially those that occur because of topographic influences can have a pronounced effect on spectral reflectance across the visible and Near Infrared portions of the electromagnetic spectrum.

1.4 Previous Tree Species Mapping Literature

Several researchers have developed methods for locating specific species within forested environments using remotely sensed data (Carter et al. 1998; Di Vittorio et al., 2009; Holmgren et al., 2008; Manjunath et al., 2013), although fewer have focused on the location of longleaf pine using multispectral satellite imagery (Van Aardt et al. 2007, Nieminen et al. 2014). Methods of spectral species identification have been established with diverse types of remotely sensed data gathered from a variety of scanners such as Light Detection and Ranging (LiDAR) (Holmgren et al. 2001), hyperspectral hand held scanners (Di Vittorio and Biging, 2009), hyperspectral imagery (Van Aardt et al 2007), aerial imagery (Waser et al. 2014), and multispectral satellite imagery (Waser et al. 2014).

Success rates of species identification using remotely sensed data have varied. Holmgren et al. (2001) combined LiDAR data with multispectral imagery to identify individual species and compared classifications derived from both types, as well as individually. The crowns of trees were located using LiDAR, and mapped to multispectral images for extraction of spectral reflectance data. The overall classification

accuracy of the combined classification of three distinct species within the study area was 96%. Vittorio and Biging (2009) investigated the spectral identification of ozone-damaged pine needles in the Sierra Nevada, using needle samples collected in the study area. Needles were grouped based on present damage relating to various causes–green (normal), winter flock, sucking-insect damage, scale-insect damage and ozone damage– and were scanned using a visible spectroradiometer configured to measure radiation at more than 2000 wavelength channels between 350–1050 nm (Di Vittorio and Biging, 2009). Although the needles were optically identical, the high spectral resolution of the scanner operating in 2000 bands allowed for specific reflectance values to be identified for each subset of needles. Using the lab derived spectral signatures from specific wavelengths across the EMS, corresponding bands were found within Airborne Visible/Infrared Imaging Spectrometer (AVIRIS) imagery for the study area. The unique signatures found for each damage class could then be used to map the varying levels of pine health across the large study area.

Manjunath et al. (2014) gathered spectral reflectance measurements of individual tree species in the Himalaya using a field spectroradiometer, and created a spectral library containing reflectance data associated with each species. This library was used to study changes in spectral response in plants and trees due to changes in both environment and health, while allowing for accurate species identification from hyperspectral imagery of the same study area in the Himalaya. The ability of these researchers to obtain distinct spectral signatures using high spectral resolution radiometers allows for greater accuracy when classifying hyperspectral images.

Using aerial imagery with a narrow array of spectral bands centered at 675, 698, and 840 nm, Carter et al. (1998) attempted to quantify the spread of the southern pine beetle within a mixed forest of conifer and hardwood, based on tree health indices related to the infestation of this invasive species. Their research allows for the location of pines within a mixed stand, while providing an early warning for the spread of the pests using spectral reflectivity. Although most outbreaks can be easily identified using multispectral scanners, the researchers found it moderately difficult to classify some trees due to the variability in leaf chlorophyll contents within the same species.

1.5 Thesis Outline and Objectives

Three stands of longleaf pine have been mapped and examined through field expeditions in the UNF. Two sites contain montane longleaf communities with individuals dating to the early 1700s (Patterson and Knapp 2016a) growing along steep, southerly slopes. The third site contains a community of longleaf growing in an area with minimal topographic variation (<20 m) and as such, has been classified with a piedmont-class distinction. Finding additional undocumented montane longleaf stands, such as the Fraley Grove stand documented in Montgomery County, NC in 2016 has proven to be difficult due to travel costs to remote locations within the forest, negotiating the steep terrain where remnant old-growth longleaf may exist, and the low rate of success on many investigatory trips.

The overarching purpose of this research is to determine if longleaf pine canopies reflect incoming electromagnetic radiation in a way that is measurably different from loblolly and shortleaf pine, both of which are present in the Uwharrie National Forest,

thereby allowing for the remote classification and mapping of these a large geographic area. Additionally, this study investigates spectral differences that may be present between the two class distinctions of longleaf, montane and piedmont, aiding in the location of rare montane habitats. A methodology for identifying spectral dissimilarities between tree species has been developed through the analysis of high spatial resolution, multispectral satellite gathered by the WorldView-2 sensor. This imagery, coupled with topographic datasets derived from LiDAR, was used to identify differences in spectral reflectance signatures that will help to classify individual canopies of longleaf pine within the National Forest with high accuracy (>90%).

Through the remote investigation of both montane and piedmont stands of longleaf pine in the Uwharrie National Forest and adjacent holdings, a better understanding of the spectral reflectance properties of the species can be gleaned, which will aid in future attempts to map longleaf pine across large geographic areas with possible montane populations. This study evaluates the viability of using multispectral imagery to: 1) isolate specific spectral characteristics to aid in the differentiation of three pine species across the UNF, 2) determine if the two class distinctions of longleaf pine possess unique spectral characteristics; 3) investigate the influence of topography and canopy height on longleaf canopy reflectance; and 4) devise a classification methodology for mapping the three species of southern pine (i.e., loblolly, longleaf, and shortleaf) in the UNF.

CHAPTER II

CONCEPTUAL FRAMEWORK AND METHODOLOGY

2.1 Discussion of Study Areas

The UNF is comprised of 20,640 hectares located in Montgomery, Randolph and Davidson Counties (Figure 2.1). The forest contains scattered longleaf pine woodlands, while shortleaf pine woodlands, loblolly plantations, dry oak-hickory forests, mafic hardpan woodlands and xeric forests are more common (USDA, 2012). Three study areas within the UNF, two containing montane communities of longleaf pine, and the third containing piedmont longleaf growing on a tract of land with low topographic relief have been located within the forest (Figure 2.2). Subsequent analyses will be focused on longleaf, shortleaf and loblolly pine growing in these areas to determine if spectral differences can be quantified to aid in the differentiation and digital mapping of the three pine species. Additionally, longleaf samples from all three sites will be compared to determine if reflectance properties vary between sites of low and high topographic prominence. Once spectral sampling in these areas has provided enough data for successful tree species classification, the resulting spectral data will be applied a larger subset of the UNF contained within the satellite imagery to locate other potential stands of montane and piedmont longleaf pine.

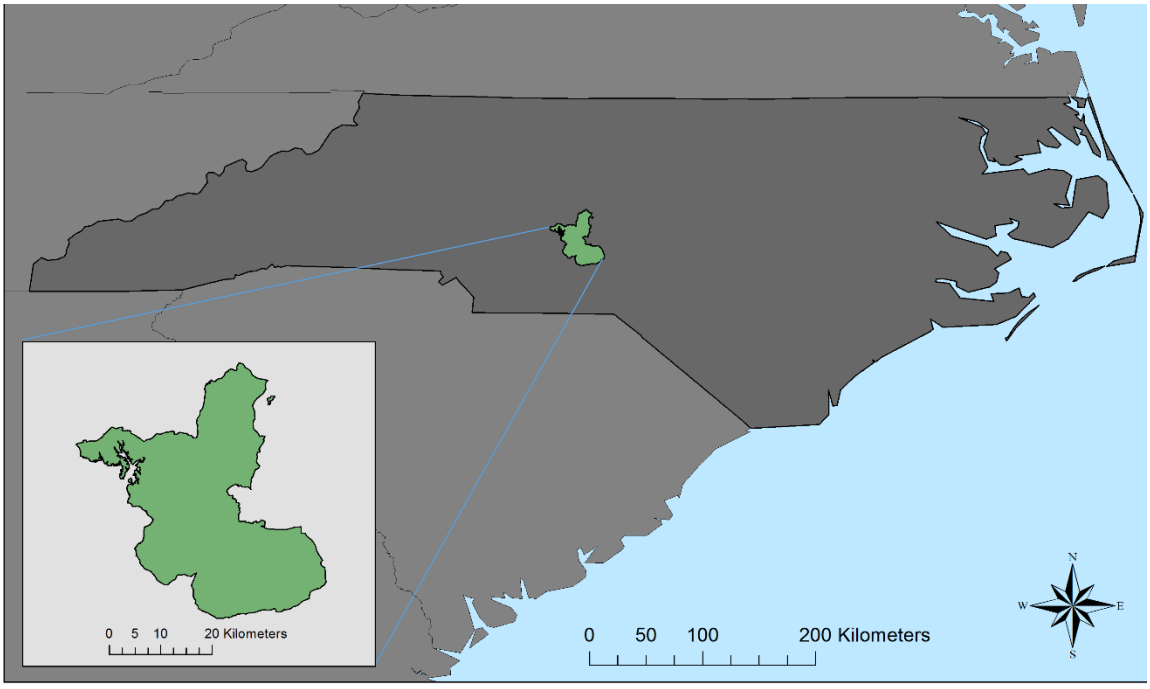

Figure 2.1. Inset Map Denoting Location Of The Uwharrie National Forest Within Central North Carolina.

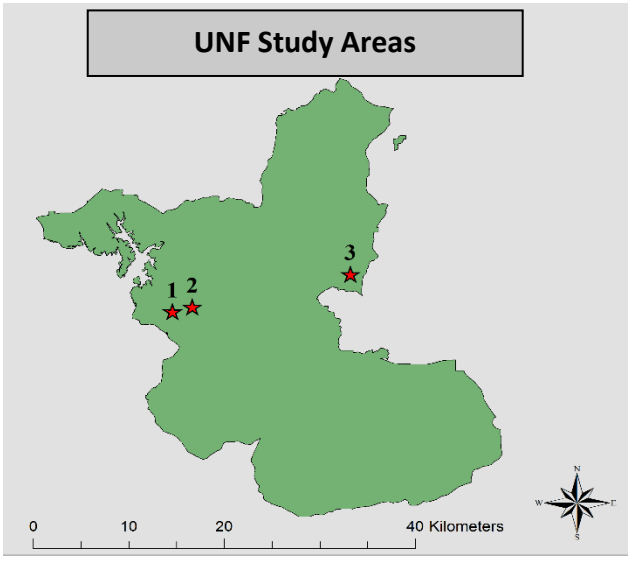

Figure 2.2. Study Areas Within UNF Denoted by Stars. 1. Fraley, 2. Goldmine, 3. Nichols

The first study area (Figure 2.3), located along Fraley Grove (Fraley), includes 235 hectares located within the center of the Uwharrie Mountains (35.352° N, 80.024° W), and contains vegetated uplands comprised of oaks and pines. The elevations range from 133.5 m to 210 m, with slopes ranging from 0° to greater than 65°. During field expeditions conducted by the Carolina Tree Ring Science Laboratory (CTRSL), montane longleaf pine mixed with hardwood species have been located along south-facing slopes and ridgelines. The second study area (Figure 2.3) is located (35.416° N, 80.036° W) along Goldmine Branch (Goldmine), 2.5 km NW of the first study site, and comprises an area of 75 hectares with similar aspect, slope and elevational characteristics of Fraley. The species composition is similar to Fraley, containing both hardwoods and montane longleaf pine along south-facing slopes. The Nichols Tract (Nichols) is the final study area (Figure 2.3) and was used to calibrate the spectral analysis for the other two areas because of its uniform elevation (< 15 m variability) and ease of access for *in situ* observations. Nichols is a 40-ha tract owned by the North Carolina Zoo located (35.456° N, 79.872° W) in Montgomery County, 17 km west of Fraley and contains a mix of piedmont longleaf, loblolly and shortleaf pine, eastern red cedar and several types of hardwoods.

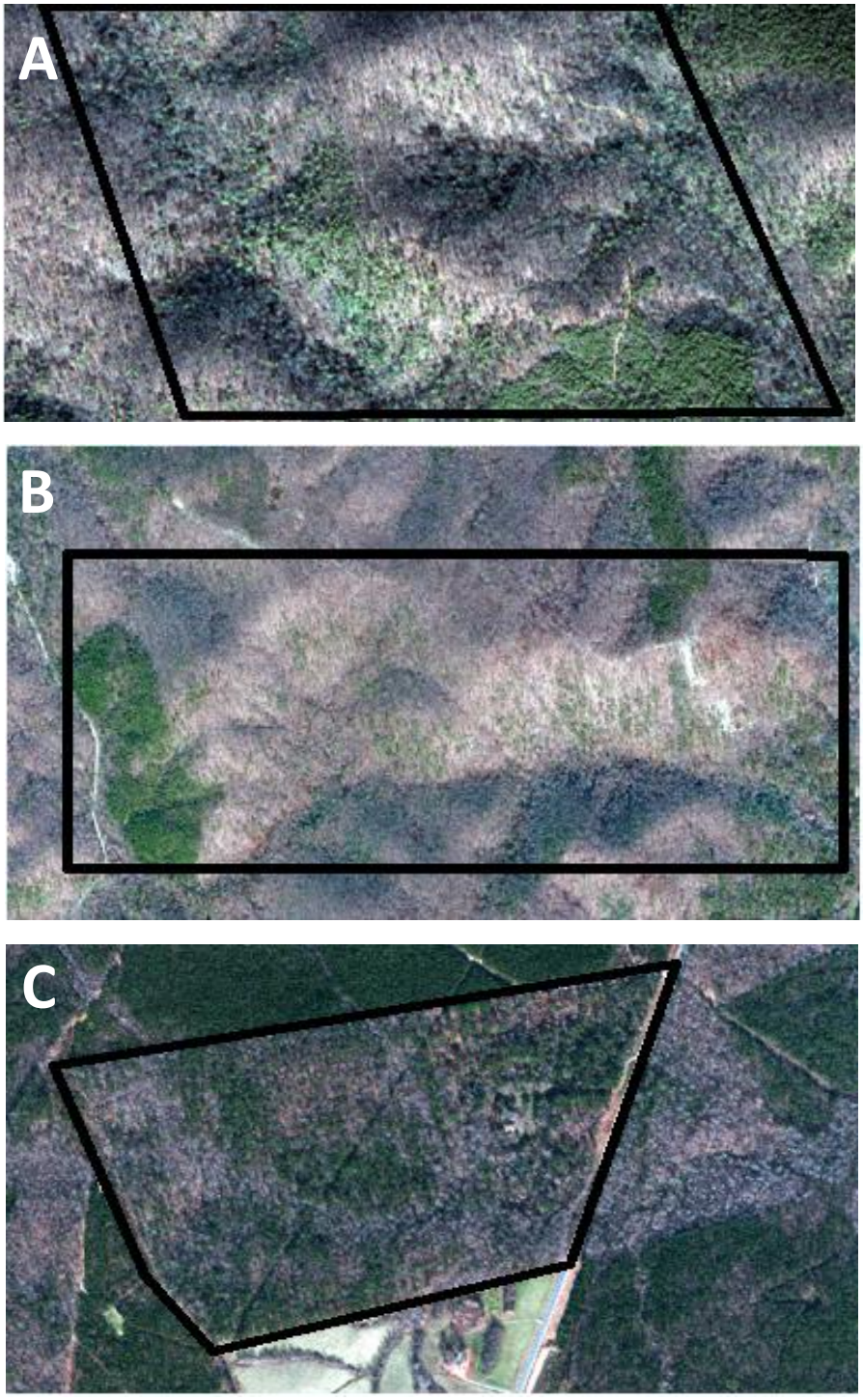

Figure 2.3. WorldView-2 Imagery Of Three Study Sites. A. Fraley Grove, B. Goldmine Branch, C. Nichols Tract. Imagery Was Acquired In December 2011.

2.2 Data Sources and Collection

Longleaf pine were sampled from three sites during winter 2016 and spring, 2017 to collect morphological and spectral data from 51 piedmont and 109 montane longleaf pine located along Fraley Trail, Goldmine Branch and within Nichols Tract. The trees were given ID numbers, and data relating to their diameter, height and canopy structure were recorded for each of the mature trees. Each sampled tree was given GPS coordinates and corresponding canopies were subsequently mapped within the satellite imagery across the tree image datasets. During the research trips, observations were made about the forest composition along the trail, noting the dispersal of individual shortleaf and loblolly pines so their location could also be mapped within a satellite image of the study area. A total of 150 shortleaf pine and 130 loblolly pine were geolocated within the three study sites.

High spatial-resolution Worldview-2 satellite imagery containing eight spectral and one panchromatic band (Table 2.1) across the visible and near-infrared portions of the electromagnetic spectrum was obtained from the Digital Globe Foundation in November 2016. The imagery was captured by the WorldView-2 satellite during leaf-off conditions on December 13th 2011. This acquisition date was selected for this study to limit the presence of deciduous leaves within the imagery, which may obscure individual longleaf crowns. The imagery spans an area of 16,182 hectares (160 km^2) within the UNF (36% coverage) and adjacent areas.

Table 2.1. Summary Of Eight Multispectral And One Panchromatic Band Contained Within WorldView-2 Imagery, As Well As Corresponding Wavelengths For Each Band.

Band Name	**WorldView-2**
Panchromatic	450-800 nm
Coastal Blue	400-450 nm
Blue	450-510 nm
Green	510-580 nm
Yellow	585-625 nm
Red	630-690 nm
Red Edge	705-745 nm
NIR-1	770-895 nm
NIR-2	860-1040 nm

Light Detection and Ranging (LiDAR) datasets were gathered from NC One map's geospatial portal. LiDAR data was collected by an airborne laser scanner during leaf-on conditions in Spring 2014, and has a reported point density of two returns per square meter. The LiDAR point clouds were processed in *ArcMap* 10.2.2 to create digital models of the terrain and overlying vegetation structure.

2.3 Development of Digital Models

Using *Arcmap,* LiDAR data were processed to create digital models of the study area representing elevations, slopes and aspects, as well as tree-canopy heights and extents. Layer files were created that contained different classes of returns from the initial acquisition. The first layer is the second class of the laser pulses to the sensor, and

is used to create models of the ground surface (Chen et al. 2012). These data produced a digital elevation model (DEM) of the study area (Figure 2.4).

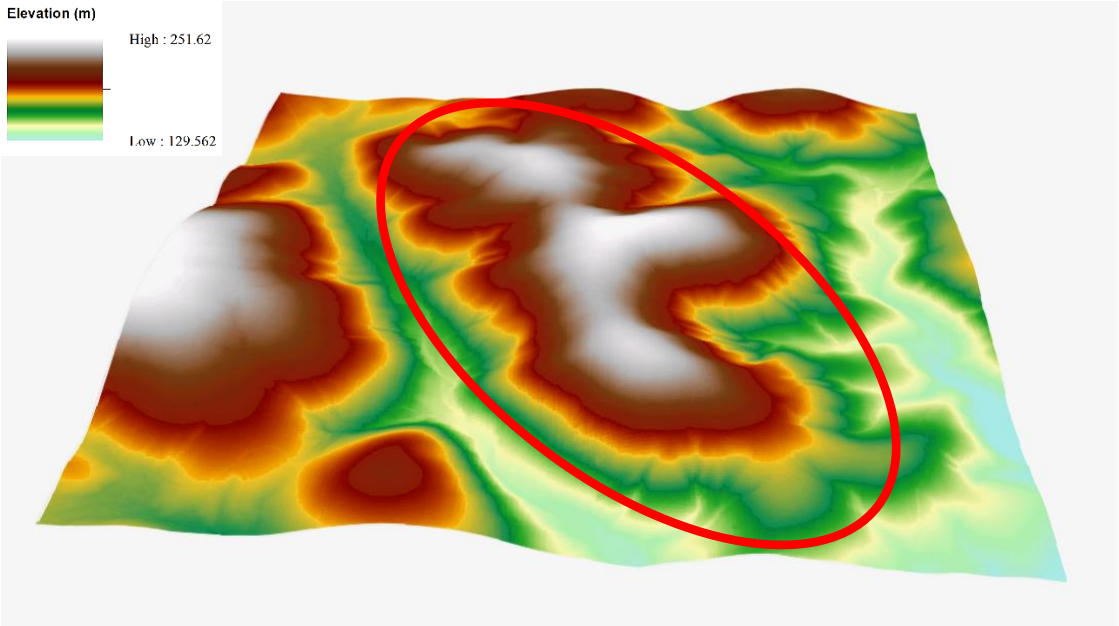

Figure 2.4. Digital Elevation Model (DEM) Of Fraley Grove Study Site. Positioned In *Arcscene* To Show Third Dimension. Red Circle Denotes Fraley Study Area.

The second process created a digital surface model (DSM) of the area using ground return points from classes 1, 3, 4 and 5. This selection of points is denoted as the "first return", as it is generally represented by tree canopies and buildings that are the first to reflect the laser pulses back to the sensor (Estornell et al. 2012) (Figure 2.5). Using the raster calculator function, DEM values for each pixel were subtracted from DSM values for the same pixels, producing a normalized DSM, which in this study is called the canopy height model (CHM), which contains tree height values for all vegetation in the study area.

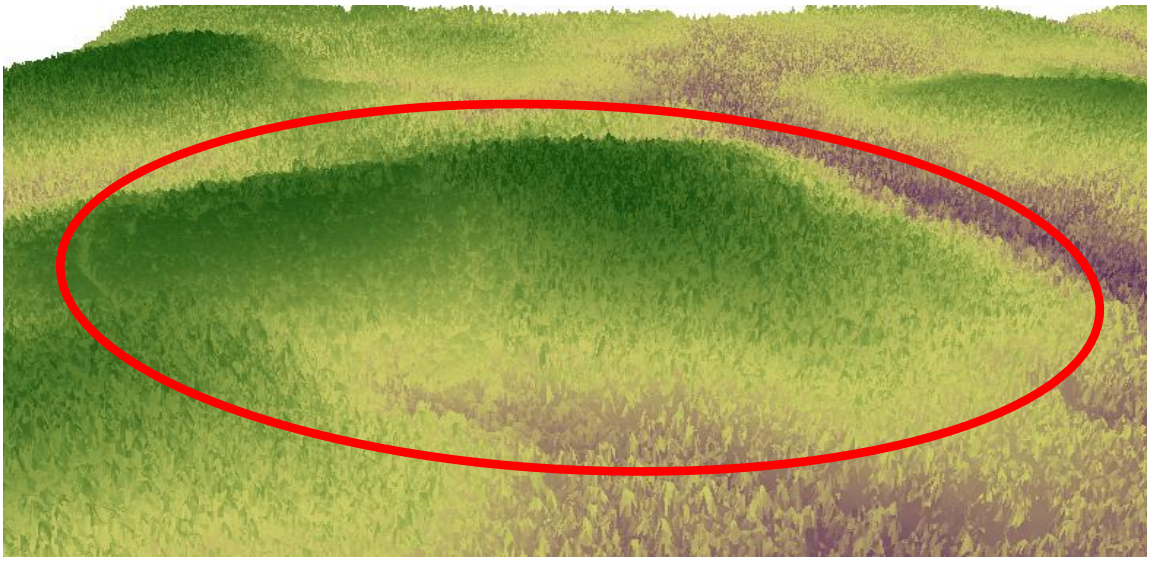

Figure 2.5. Digital Surface Model Showing Tree Canopies Derived From First Return Of Lidar. This Image Shows The Southwest Slope Of Fraley Grove, Circled In Red.

Using the derived DEM, Spatial Analyst tools within *Arcmap* were utilized to create a digital representation of slopes within the study area (Figure 2.6), which range in angle from 5–29^{o}. Utilizing the same DEM, the Slope tool was used to determine the aspect of each slope, with values ranging from 0–360^{o} (Figure 2.7). The DEM, slope, aspect and CHM were then combined into a dataset that could then be added into subsequent combination datasets with WV-2 imagery.

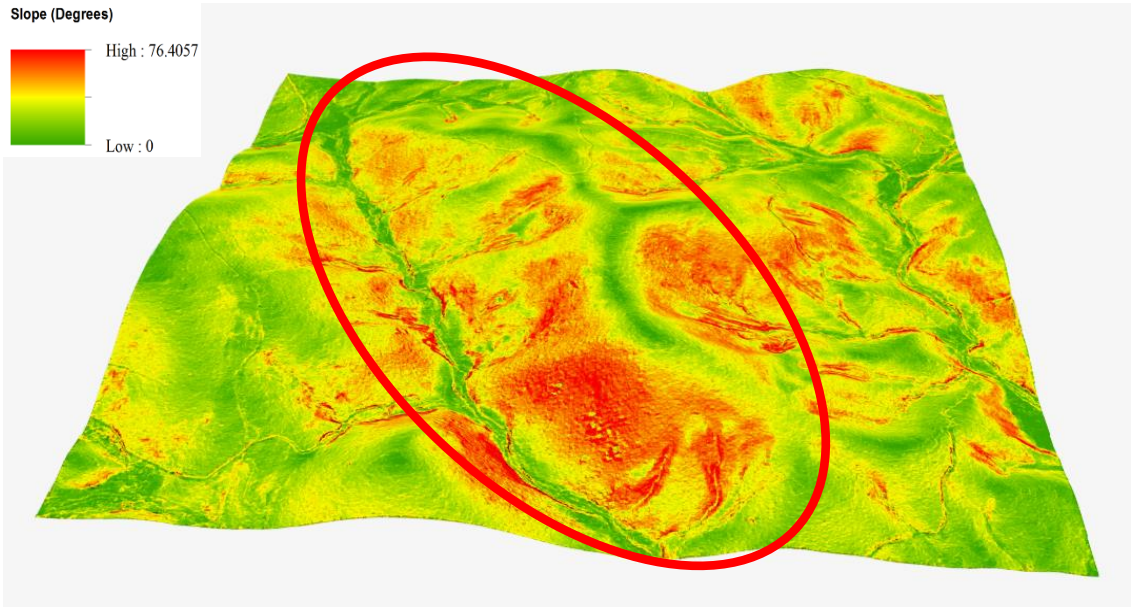

Figure 2.6. Digital Model Of Slopes Throughout The Study Area With Fraley Circled In Red. Steep Slopes Along Southern Face Of Fraley Grove Are Shaded With Red.

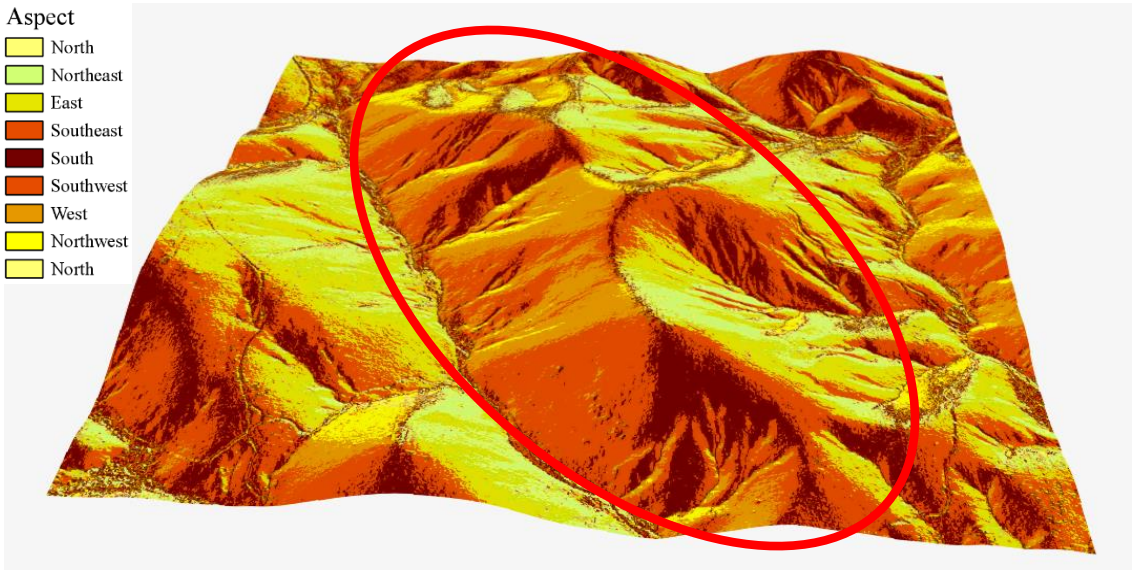

Figure 2.7. Digital Model Of Aspect Throughout The Study Area With Fraley Circled In Red. Darker Slopes Have Southerly Aspects, And Lighter Slopes Have Northerly Aspects.

2.4 Preprocessing of WorldView-2 Imagery

The imagery dataset used in this research contained a set of multispectral bands as well as a separate panchromatic band. The multispectral and panchromatic images were orthorectified within ENVI 5.3 *(Exelis Visual Information Solutions, Boulder, Colorado)* using the ground control point file contained with the imagery metadata, as well as a 5-m digital elevation model (DEM) of the study area developed from a LiDAR point cloud of the study areas. The orthorectification process used a Cubic Convolution Image resampling method with output pixel sizes determined by the input image.

Once the images had been successfully orthorectified, the multispectral imagery datasets were radiometrically calibrated to ground surface reflectance using the Empirical Line Calibration discussed by Jensen (2005). The resulting multispectral image raster was then atmospherically corrected using ENVIs FLAASH tool per the date and time of acquisition, which allowed for the program to determine the solar elevation and azimuth, correcting for atmospheric interference of particles and gasses that can influence the reflectance within an image (Jensen 2005). The corrected multispectral image was then pansharpened using the simultaneously gathered 0.5 m panchromatic image to increase the spatial resolution from 2 m to 0.5 m (Aguilar et al. 2013). The resulting calibrated, atmospherically corrected, rectified and pansharpened dataset was then used for object-based image analysis.

2.5 Spectral Indices

Although the eight spectral bands contained within the WorldView-2 imagery were suitable for differentiating between pines and hardwoods within the study areas,

significant spectral overlap between longleaf, shortleaf and loblolly pines did not produce accurate classifications during preliminary tests. In order to help distinguish between the spectrally similar species in the imagery, spectral vegetation indices were calculated using two or more of the eight multispectral bands within the image datasets (Table 2.2). Calculation and inclusion of band ratios like the Normalized Difference Vegetation Index (NDVI) can reveal information pertaining to plant health, and can also improve the ability of classification methods to discriminate between species with similar spectral reflectance (Haboudane et al. 2004, Sripada et al. 2006, Shamsoddini et al. 2013). A total of eight spectral indices were chosen from 38 available indices within the ENVI program based upon visual inspection and referenced literature. The indices were incorporated into the imagery dataset used for subsequent classification assessment.

Table 2.2. List Of Eight Spectral Indices Calculated From Worldview-2 Imagery Gathered On December 13, 2011. Abbreviations For Each Index Are Listed In First Column, The Full Name Is Listed In The Second Column, The Formula To Derive The Indicies Is Listed For Each In The Third Column, And The Reference For Each Is Listed In The Fourth Column.

Abbreviation	Spectral Index	Formula	Reference
(DVI)	Difference vegetation Index	$DVI = NIR - RED$	(Tucker 1979)
(MNLI)	Modified Non-Linear Index	$MNLI = ((NIR^2 - RED) * (1 + L))/(NIR^2 + RED + L)$	(Yang et al. 2008)
(NLI)	Non-Linear Index	$NLI =((NIR^2 - RED))/((NIR^2 + RED))$	(Goel and Qin 1994)
(GDVI)	Green Difference Vegetation Index	$GDVI = NIR - GREEN$	(Sripada, R., et al. 2006)
(GNDVI)	Green Normalized Difference Vegetation Index	$GDVI = (NIR - GREEN)/(NIR + GREEN)$	(Gitelson and Merzlyak 1998)
(NDVI)	Normalized Difference Vegetation Index	$NDVI = ((NIR - RED))/((NIR + RED))$	(Rouse et al. 1973)
(TDVI)	Transformed Difference Vegetation Index	$TDVI = \sqrt{0.5 + (NIR - RED)/(NIR + RED)}$	(Asalhi and Teillet 2002)
(TCARI)	Transformed Chlorophyll Absorption Reflectance Index	$TCARI = 3[(R_{700} - R_{670}) - 0.2(R_{700} - R_{550})(R_{700}/R_{670})]$	(Haboudane et al. 2004)

2.6 Shadow and Vegetation Masking

A raster mask was created for the image datasets so that the only pixels analyzed for spectral analysis and classifications were contained within the sunlit portions of conifer tree crowns (Xiao et al. 2004). The mask was developed using the Modified Non-Linear Index that had been calculated using the WorldView-2 spectral bands. Visual inspection of the MNLI raster revealed that conifer crowns have higher reflectance for

this index than do non-conifer pixels in the imagery. This masking process was completed through several iterations to ensure that pixels known to contain shadows, as well deciduous trees, understory vegetation, bare earth, water and roads were not included in further analysis. Within the binary mask, pixels containing MNLI values of less than 1.46 were assigned a value of 0, while all values greater than this threshold, which corresponded to pine canopies, were assigned a value of 1 (Figure 2.8). Only pixels with a mask value of 1 were included in subsequent analysis.

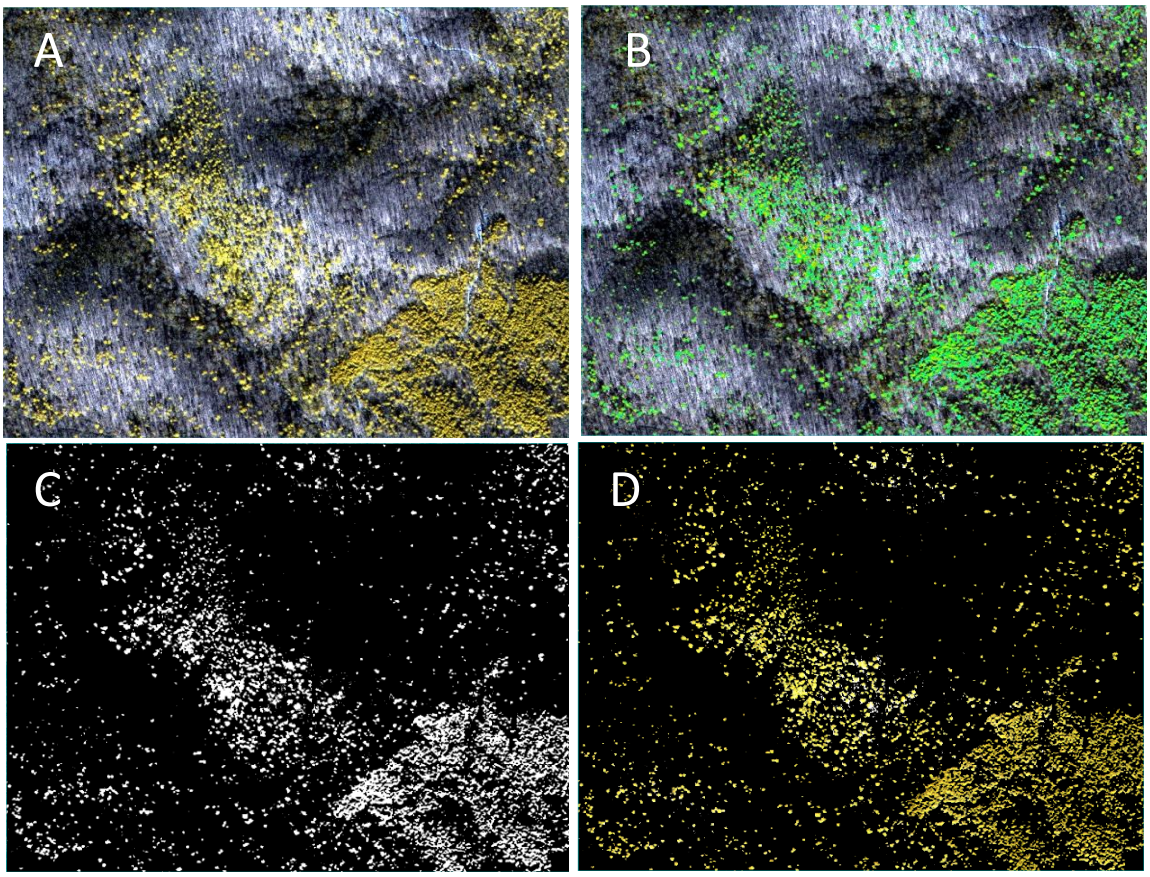

Figure 2.8. Development Of Raster Mask To Isolate Only Sunlit Tree Crowns. A. False Color Image Of Fraley Grove. B. Raster Color Slice Produced In ENVI Showing MNLI Values Within Fraley Study Area. C. Binary Raster Mask Created In ENVI Using MNLI Threshold. D. Applied Raster Mask Showing Only Sunlit Tree Crowns.

2.7 Spectral Analysis of Tree Canopies

2.7.1 Spectral Relationships with External Influences

Although spectral reflectance in vegetation can be influenced by the physical and biochemical characteristics of leaves and needles (Sims and Gamon 2002), this study investigates how external variables such as topography and canopy height can influence spectral reflectance properties for longleaf pine. Analysis of external influences on spectral reflectance was completed using 109 montane and 51 piedmont longleaf across the three study sites. Descriptive statistics for the 160 longleaf canopies were calculated, resulting in minimum, maximum, mean and standard deviation pixel values for each canopy, with values for each of the eight spectral bands in the imagery. Pixel values for each of the descriptive statistics were calculated from each tree's reflectance, and compiled for analysis in IBM's SPSS statistical software (IBM 2006).

Testing of the reflectance relationships between topographic and tree height variables was completed using a dataset of raster layers which included the eight WorldView-2 multispectral bands, as well as elevation, slope, aspect and tree height rasters. The December imagery was stacked with the four other layers to create a 12-band image file, and then masked using the MNLI binary masking process used above. Pixel values were extracted from each of the 160 longleaf canopies across the three study sites, and descriptive statistics were calculated for each layer in the dataset including values for the eight spectral bands, as well as elevation, slope, aspect and tree height.

To determine which of the four variables were significantly correlated with canopy reflectance, a Pearson product-moment correlation was implemented, which

measured the strength of linear association between reflectance across the eight WorldView-2 bands and the external variables included in the dataset (topographic variables and canopy height). Correlation coefficients produced from this analysis were compared to determine the strength of individual variables to explain the variance in spectral reflectance.

2.7.2 Spectral Relationships Between and Among Species

To determine if spectral differences exist between the tree species throughout the study areas, samples of competing pine species were also sampled and analyzed. 130 loblolly pine and 150 shortleaf pine canopies were located throughout the three study sites, mapped in the masked satellite imagery and then each canopy was sampled for spectral reflectance values. Descriptive statistics were calculated for each tree of both species, and added to the dataset containing canopy values for the 160 longleaf pine. A Mann-Whitney non-parametric test of means (Guo and Guo 2014) was implemented over three iterations. The first test compared reflectance values between longleaf and loblolly, the second compared values for shortleaf and longleaf, and the third tested reflectance values between shortleaf and loblolly for each of the eight bands in the imagery. Significance values derived from this test that are less than or equal to 0.05 are statistically significant, and indicate that reflectance between the species was significantly different for the band being tested.

Additionally, to determine whether spectral differences were present between montane and piedmont longleaf samples, a Mann-Whitney non-parametric test of means was implemented using the previously derived reflectance statistics from 54 montane

samples gathered at Goldmine and 54 piedmont samples gathered from Nichols, using site location as the independent variable.

2.8 Image Classification

2.8.1 Object-Based Image Classification

Digital image classification techniques can be used to group pixels based on their specific spectral reflectance into user defined groups to isolate land cover types (Jensen 2007). Typically, these groups consist of forested cover, urban areas, grassland, and agricultural land, each represented by pixels within an image with similar reflectance values. Geographic information systems like ENVI and Arcmap have tools that aid in the creation of classifications from digital images. Within these programs, two types of classifications can be used to identify and group pixels in the image, although only supervised and unsupervised are discussed here. Unsupervised classifications group pixels based on reflectance properties, as determined by the user-defined groupings or clusters. By selecting the number of groups and the specific wavelengths or bands for the software, the image is separated into groups of similar reflectance (Jensen, 2007).

Supervised pixel-based classifications require a user to select classes; areas in an image with homogeneous land cover, such as bodies of water, agricultural fields, built-up areas, or specific tree canopies that are manually delineated with vector polygons. Using spectral information gathered from each pixel in each chosen class, the software can identify land-cover classes throughout the image based on the measured spectral reflectance of individual pixels contained within the chosen training sites. The

classification algorithm groups the pixels according to the spectral signatures for each class, and creates a raster file showing the clusters within the image (Jensen, 2007).

Pixel-based classification procedures are not well suited for discrimination between species with similar spectral properties as so-called "salt and pepper' effects emerge due to the high variation in reflectance between adjacent pixels that can exist within a tree's canopy due to shadowing, needle length variation and canopy health.

As an additional measure for classifying objects with similar spectral characteristics, a supervised, object-based image analysis (OBIA) can be implemented, which creates image segment boundaries, which are discrete regions, created by the software within digital imagery based on image objects with similar characteristics relating to reflectance, texture or shape (Blaschke et al. 2008). This segmentation process has parameters that can be adjusted to minimize or maximize sensitivity to reflectance and object size. The user then creates training samples by selecting the segmented polygons in the image that correspond to a specific land cover type.

2.8.2 Classification Methodology

The classification technique used in this paper is an object-based supervised classification. Despite significant differences in reflectance between the three-pine species across eight spectral bands, initial classification attempts were not able to accurately differentiate between the species, requiring more spectral data to be included in the classification. The following classifications were implemented on a dataset containing eight WorldView-2 bands, as well as eight previously calculated spectral indices. Again, the image had been masked per MNLI values so that the only pixels

remaining in the image were composed of the sunlit portions of conifer tree crowns. An individual classification was completed for each of the three study sites, and then a fourth classification was implemented for a larger area within the UNF using training samples selected from all three locations.

The first step in the procedure grouped pixels within the image based on similar reflectance values, and was adjusted to focus the *segment* polygons around entire tree canopies (Figure 2.9). The next step required the selection of samples that pertain to the classes present within each study site, which in this case were the three species of pine. At each of the three study sites, 25 longleaf, shortleaf and loblolly pine canopies were selected from the segmented image as training samples to train the classification algorithm to differentiate between the segmented image objects. Twenty-five other located samples for each species were retained to calculate the accuracy of each classification. For the larger area, 50 training samples from each species were selected for the classification.

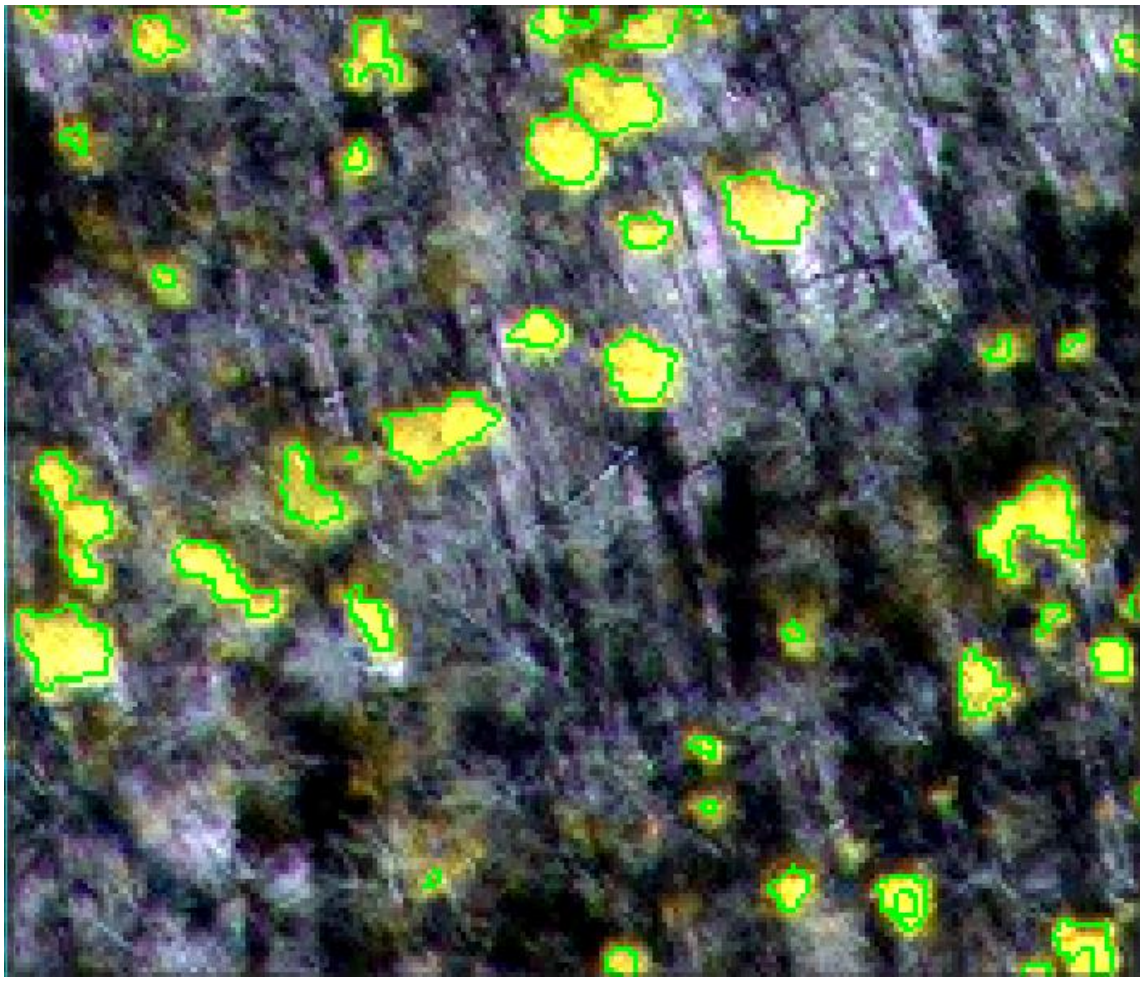

Figure 2.9. Image Segments Developed By The ENVI Feature Extraction Segmentation Process. Shown Encompassing Entire Sunlit Portions Of Tree Crowns. Image Is A False Color Representation, Using Bands 7, 6 And 5 Substituted For Red, Green And Blue Respectively.

Once the training samples were selected for each site-classification, a Support Vector Machine (SVM) classification method was implemented to group the image objects or segments into classes based upon spectral reflectance values across the 16 bands. This classifier incorporates spectral data relating to mean, minimum, maximum and standard deviation for each class, while also compiling data relating to texture, size

and shape of each of the image objects for each class. The resulting output from this classifier is a raster image containing locations across the study site that have been classified based on the classification parameters. Four total classifications were implemented, and their accuracies were then assessed.

2.8.3 Accuracy Assessment

To test the accuracy of each classification implemented at the three sites as well as across the larger area surrounding Fraley and Goldmine, ground-truth data relating to the locations of each geolocated tree canopy were compared to the classification image to determine if each tree was correctly classified. A stratified random sampling method was used to select ground truth points from each study site (Jensen, 2007). For the three sites 80 samples were randomly selected from the 150 located trees for each site, with 25 set as the minimum number of samples for each class (longleaf, shortleaf and loblolly) while a minimum of 50 were chosen for the larger area. These chosen samples are listed in Table 2.3.

Table 2.3. Number Of Ground Truth Samples Randomly Chosen From Each Class.

Class	Fraley	Goldmine	Nichols	Larger Area
Longleaf	26	27	29	54
Shortleaf	28	25	25	59
Loblolly	26	28	26	52
Total	80	80	80	155

Accuracy assessments for image classifications are derived from error matrix tables, which are produced when ground sample regions are compared to pixel classes within classification images (Jensen 2007). Values within the matrix are derived by calculating the number of correctly and incorrectly classified pixels or objects within an image. The first value used to assess accuracy is known as user's accuracy (UA), and calculates errors of commission (Aguilar et al. 2013) by determining the number of pixels belonging to an object in one class, but have been classified as another, incorrect class. The second metric is producer's accuracy (PA), which is related to errors of omission and is calculated by determining the number of pixels relating to one class that have not been grouped within that class. Overall accuracy (OA) is calculated by dividing the number of correctly classified objects or pixels by the total number of objects or pixels. Lastly, a more robust accuracy metric that is calculated is the Kappa Statistic (KS), which evaluates how well the classification procedure performed by comparing the results to a random classification. KS values ranges from -1 to 1, with negative values denoting that the classification performed worse than random, and 1 meaning that the classification performed significantly better than normal (Jensen 2007). All four accuracy parameters have been assessed for the four classifications completed for this research.

CHAPTER III

RESULTS

3.1 Spectral Analysis Results

Analysis results of topographic influences on spectral reflectance showed significant relationships between elevation, slope and aspect for several of the WorldView-2 bands across the visible and near-infrared portions of the spectrum (Table 3.1). A significant relationship between aspect and reflectance was only present for the Green band, with a correlational coefficient of (r = 0.171, $p \leq 0.05$). Elevation had a stronger relationship with reflectance values from the 160-sampled longleaf, with the Blue and Yellow portions of the spectrum exhibiting positive correlations of (r = 0.197 and r = 0.182; $p \leq 0.05$) respectively, and coefficients of (r =0.223 and r = 0.221; $p \leq$ 0.01) for the Coastal Blue and Red bands.

Relationships between slope and reflectance were highly significant across all bands of the imagery with coefficients ranging from (r = -0.616–0.813; $p \leq 0.01$) with stronger negative relationships present in the near-infrared portions of the spectrum. The Pearson product-moment correlation procedure also revealed strong relationships between canopy height and reflectance across each of the eight bands (Table 3.2). Coefficient values range from (r = 0.371–0.657; $p \leq 0.01$) with all values significant at the 0.01 level. It was also found that tree height is significantly related to both slope (r =-0.647; $p \leq 0.01$) and elevation (r =-0.380; $p \leq 0.01$).

Table 3.1. Pearson Product-Moment Correlations Between Reflectance And External Variables: Elevation, Slope, Aspect And Canopy Height. Significant Values Are Denoted By * For ($p \leq 0.05$) And ** For ($p \leq 0.01$)

		Coastal Blue	Blue	Green	Yellow	Red	Red Edge	NIR1	NIR2
Elevation	Pearson Correlation	.223**	.197*	0.149	.182*	.221**	0.04	0.009	-0.033
	Sig. (2-tailed)	0.007	0.016	0.073	0.027	0.007	0.629	0.911	0.688
Slope	Pearson Correlation	-.627**	-.687**	-.681**	-.653**	-.616**	-.781**	-.799**	-.813**
	Sig. (2-tailed)	(<0.01)	(<0.01)	(<0.01)	(<0.01)	(<0.01)	(<0.01)	(<0.01)	(<0.01)
Aspect	Pearson Correlation	0.156	0.161	.171*	0.131	0.097	0.087	0.072	0.031
	Sig. (2-tailed)	0.058	0.051	0.038	0.112	0.241	0.293	0.383	0.704
Canopy Height	Pearson Correlation	.401**	.464**	.475**	.448**	.371**	.615**	.641**	.657**
	Sig. (2-tailed)	(<0.01)	(<0.01)	(<0.01)	(<0.01)	(<0.01)	(<0.01)	(<0.01)	(<0.01)
	N	160	160	160	160	160	160	160	160

Table 3.2. Pearson Product-Moment Correlations Between Canopy Height, Elevation, Slope And Aspect. Significant Values Denoted By ** For ($p \leq 0.01$).

		Elevation	Slope	Aspect
Canopy Height	Pearson Correlation	-.380**	-.647**	-0.027
	Sig. (2-tailed)	(<0.01)	(<0.01)	0.749
	N	160	160	160

To determine if spectral reflectance differences were present between montane and piedmont longleaf samples, the Mann-Whitney non-parametric test was implemented to compare reflectance values between a subset of longleaf sampled from the two montane stands (n=54) to the piedmont samples gathered at Nichols (n=54). Significant differences were found for reflectance across all eight bands between the two classes of longleaf ($p \leq 0.01$) (Table 3.3). To better visualize the differences in reflectance, mean reflectance values for each tree from both subsets were compiled and incorporated into two line charts (Figure 3.1). Additionally, mean reflectance was calculated for each montane and piedmont longleaf canopies in the subset, and incorporated into a third chart showing the differences in reflectance across each band in the imagery (Figure 3.2).

Table 3.3. Mann-Whitney U-Test Results For Comparison Between Montane And Piedmont Longleaf Reflectance Across The Eight Bands Of December WorldView-2 Imagery. Significance Values ($P \leq 0.05$) Are In The Bottom Row.

Test Statistics								
	Coastal Blue	Blue	Green	Yellow	Red	RedEdge	NIR-1	NIR-2
Mann-Whitney U	295.5	107.5	97	158	375.5	0	0	0
Wilcoxon W	1780.5	1592.5	1582	1643	1860.5	1485	1485	1485
Z	-8.943	-9.691	-9.728	-9.484	-8.618	-10.112	-10.115	-10.113
Asymp. Sig. (2-tailed)	0.000	0.000	0.000	0.000	0.000	0.000	0.000	0.000

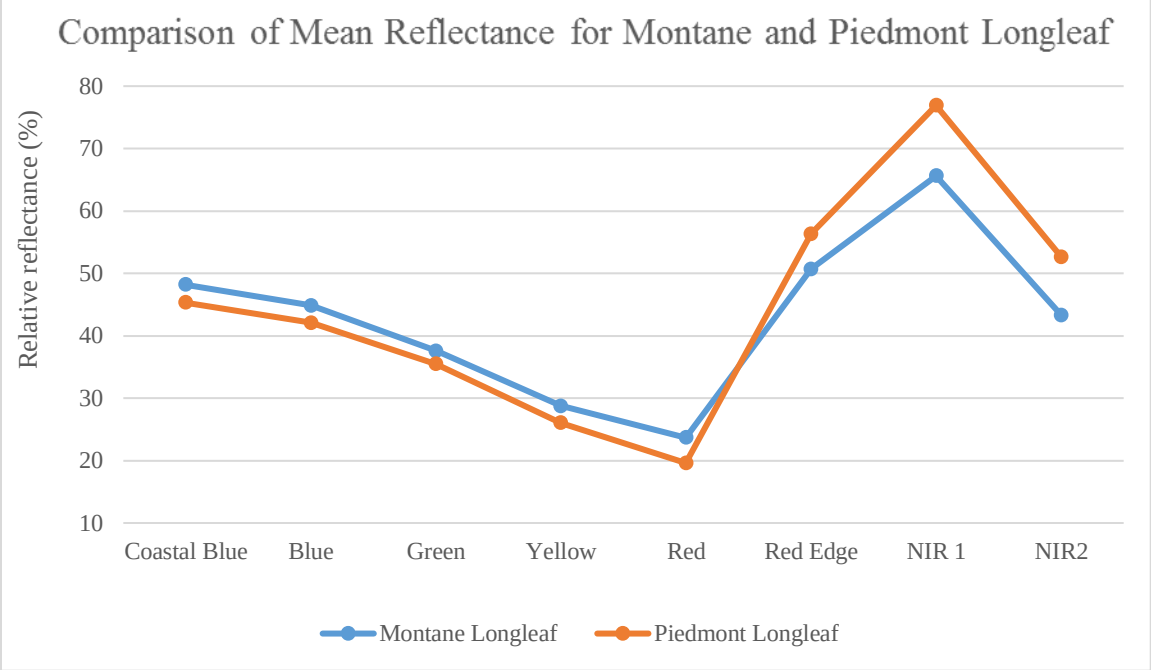

Figure 3.1. Mean Reflectance Derived From 54 Piedmont And 54 Montane Longleaf Samples Gathered From Nichols, Fraley And Goldmine.

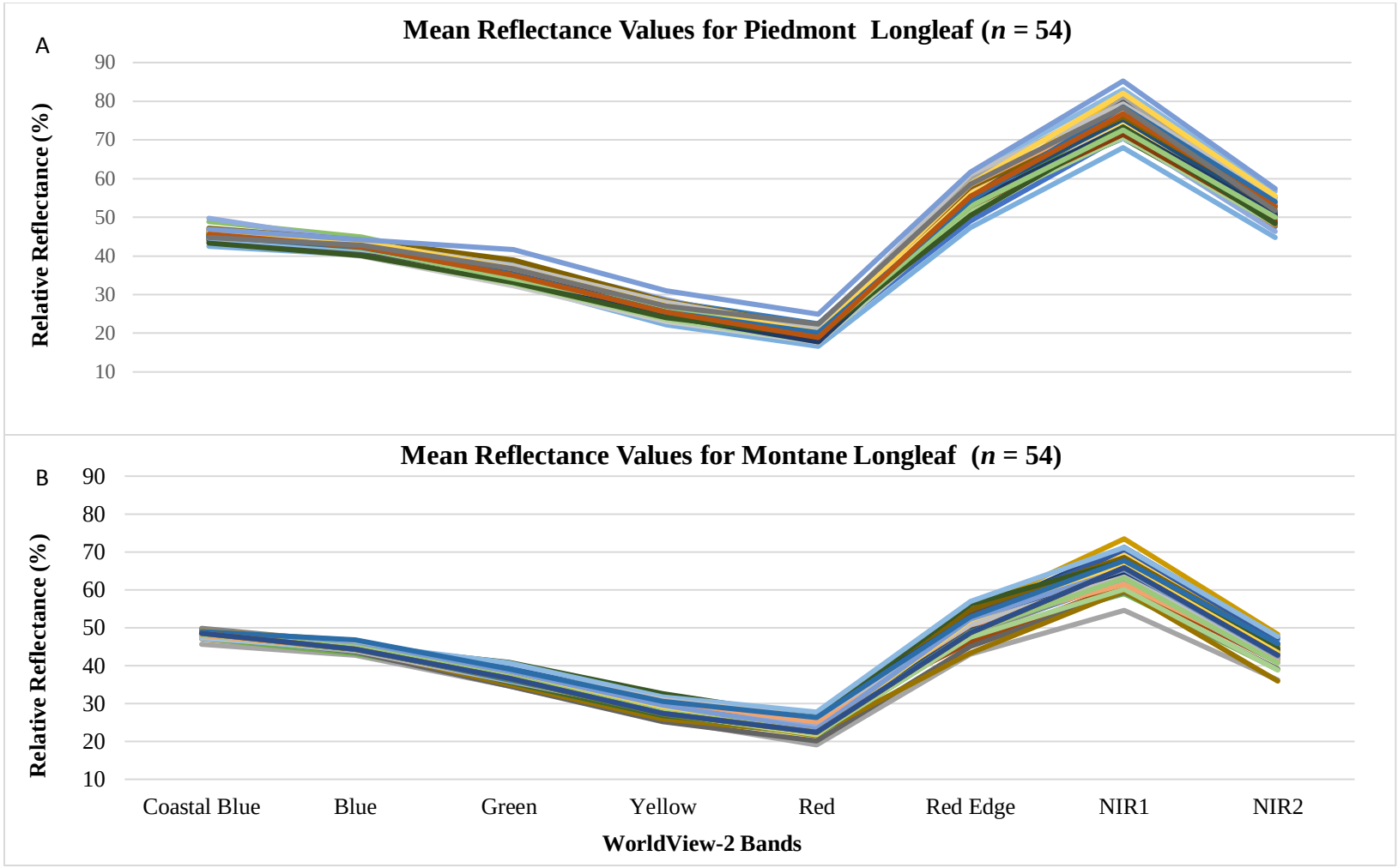

Figure 3.2. Distribution Of Mean Reflectance Values For Longleaf. A.) Subset Of Montane Longleaf Samples Gathered From Goldmine And Fraley Grove. B.) Piedmont Longleaf Gathered From Nichols Tract.

Spectral analysis results indicate that the spectral discrimination of longleaf, shortleaf and loblolly pine is possible due to the unique spectral properties of the three pine species (Figure 3.3). Mean reflectance values for the Green, Yellow, Red, and NIR-1 bands vary between samples of Longleaf and Shortleaf Pine (p <0.05) (Table 3.4). Longleaf and Loblolly pine mean reflectance differs significantly across the Green, Yellow, Red, Red Edge and NIR-2 bands (p <0.05) (Table 3.5). Additionally, spectral variations in mean reflectance from Green and Red bands were found between shortleaf and loblolly pine samples (p <0.05) (Table 3.6).

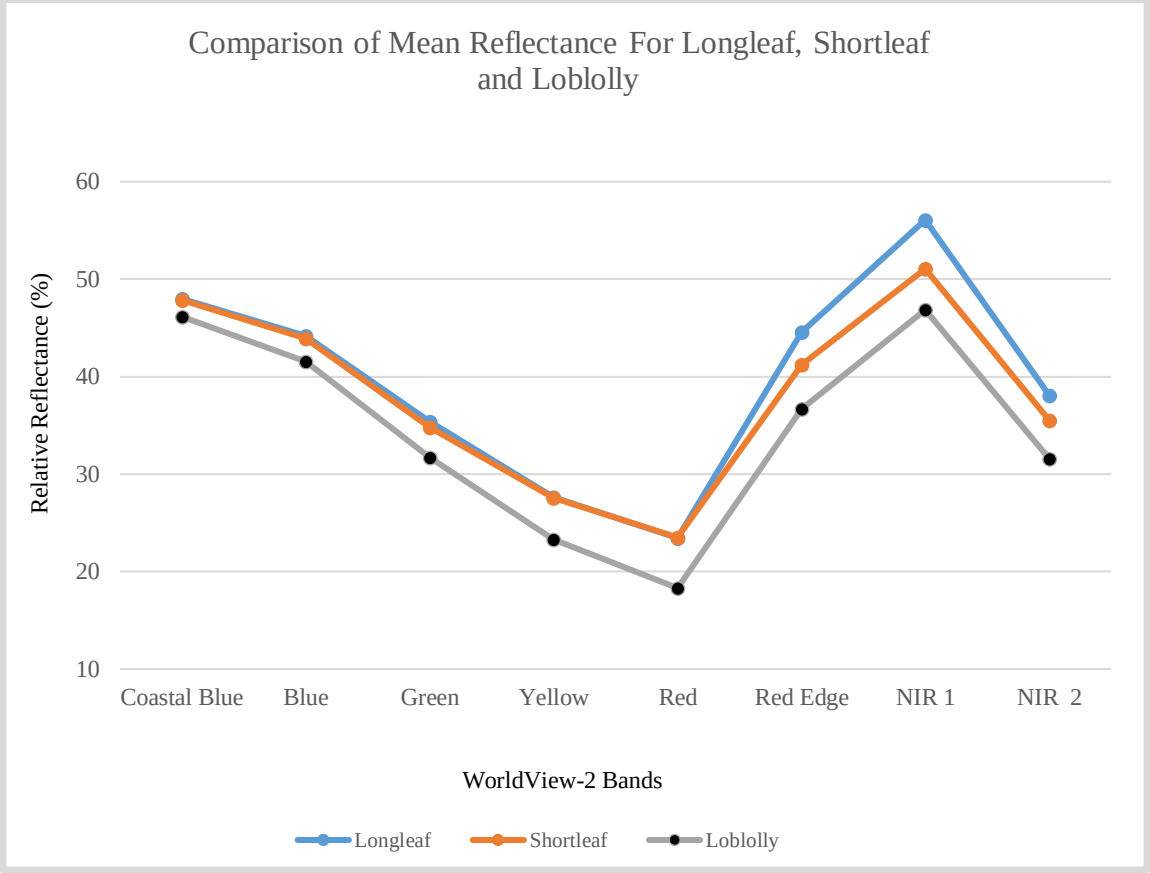

Figure 3.3. Mean Reflectance Derived From 160 Longleaf, 150 Shortleaf And 130 Loblolly Pine Samples Gathered From Nichols, Fraley And Goldmine.

Table 3.4. Mann-Whitney U-Test Results For Spectral Comparison Of Longleaf And Shortleaf Pine Reflectance. Significant Values Are Highlighted (p <0.05)

Test Statistics								
	Coastal Blue	Blue	Green	Yellow	Red	RedEdge	NIR-1	NIR-2
Mann-Whitney U	343.5	387.5	288.5	162	144	380	292	402.5
Wilcoxon W	694.5	738.5	883.5	757	739	975	643	753.5
Z	-1.47	-0.813	-2.29	-4.177	-4.446	-0.925	-2.238	-0.589
Asymp. Sig. (2-tailed)	0.142	0.416	0.022	0.000	0.000	0.355	0.025	0.556

Table 3.5. Mann-Whitney U-Test Results For Spectral Comparison Of Longleaf And Loblolly Pine Reflectance. Significant Values Are Highlighted (p <0.05)

Test Statistics								
	Coastal Blue	Blue	Green	Yellow	Red	RedEdge	NIR-1	NIR-2
Mann-Whitney U	628.5	497.5	395.5	292	168.5	404	544.5	476.5
Wilcoxon W	1223.5	1092.5	990.5	887	763.5	999	1139.5	1071.5
Z	-0.382	-1.83	-2.958	-4.103	-5.469	-2.864	-1.31	-2.062
Asymp. Sig. (2-tailed)	0.703	0.067	0.003	0.000	0.000	0.004	0.19	0.039

Table 3.6. Mann-Whitney U-Test Results For Spectral Comparison Of Loblolly And Shortleaf Pine Reflectance. Significant Values Are Highlighted (p <0.05)

Test Statistics								
	Coastal Blue	Blue	Green	Yellow	Red	RedEdge	NIR-1	NIR-2
Mann-Whitney U	3.929	7.574	0.04	0.734	0.04	5.243	13.121	7.03
Wilcoxon W	1	1	1	1	1	1	1	1
Z	0.047	0.006	0.841	0.391	0.841	0.022	0	0.008
Asymp. Sig. (2-tailed)	3.929	7.574	0.040	0.734	0.040	5.243	13.121	7.030

3.2 Classification Accuracy and Results

Overall classification accuracy for the four classified sites ranged between 88.81–92.54 %, demonstrating highly accurate mapping of the three pine species. Kappa Coefficients ranged from 0.78–0.85, indicating that the classifications were significantly different from random (Table 3.7). While overall accuracies were high for the three species, errors of commission for longleaf pine were high at some sites, with user accuracies of 92.11% for Fraley (Figure 3.4), 86.91% for Goldmine (Figure 3.5) and 96.85% for Nichols Tract (Figure 3.6), with a UA of 78.53 for the larger area in the UNF (Figure 3.7). Errors of omission for Fraley were moderate with close to 88% (Table 3.8) with producer's accuracies ranging from 93.80% for Goldmine (Table 3.9), 80.12% for Nichols (Table 3.10) and 79.53% for the larger classified area. Accuracies for longleaf pine were lower than the two competing pines throughout the four sites (Table 3.7), suggesting that variations in spectral reflectance for longleaf may be greater between sites, limiting the ability of the classifier to identify all samples present in the imagery.

After completing the classification on the larger area, several locations were noted to contained tree canopies classified as longleaf pine. Five sites were chosen for further investigation in areas with relatively steep southerly slopes (Figure 3.7). After visiting these sites to check the accuracy of the classification, four of the five sites contained stands of either loblolly or shortleaf pine. The fifth site was located on private property, and was therefore not investigated further.

Table 3.7. Accuracy Results For Four Classifications Completed Within The UNF. A. User's Accuracy. B. Producer's Accuracy. C. Overall Accuracy And Kappa Statistics.

A	Producer's Accuracy (%)		
	Longleaf	Loblolly	Shortleaf
Fraley	86.45	N/A	91.82
Goldmine	93.80	77.30	95.77
Nichols	80.12	97.25	97.61
Larger Area	78.53	90.97	94.02
B	User's Accuracy (%)		
	Longleaf	Loblolly	Shortleaf
Fraley	92.11	N/A	85.98
Goldmine	86.91	94.90	86.02
Nichols	96.85	99.97	80.99
Larger Area	78.53	90.97	94.02
C	Overall Accuracy		Kappa Statistic
Fraley	89.00 %		0.78
Goldmine	88.81 %		0.83
Nichols	92.54%		0.88
Larger Area	91.67 %		0.85

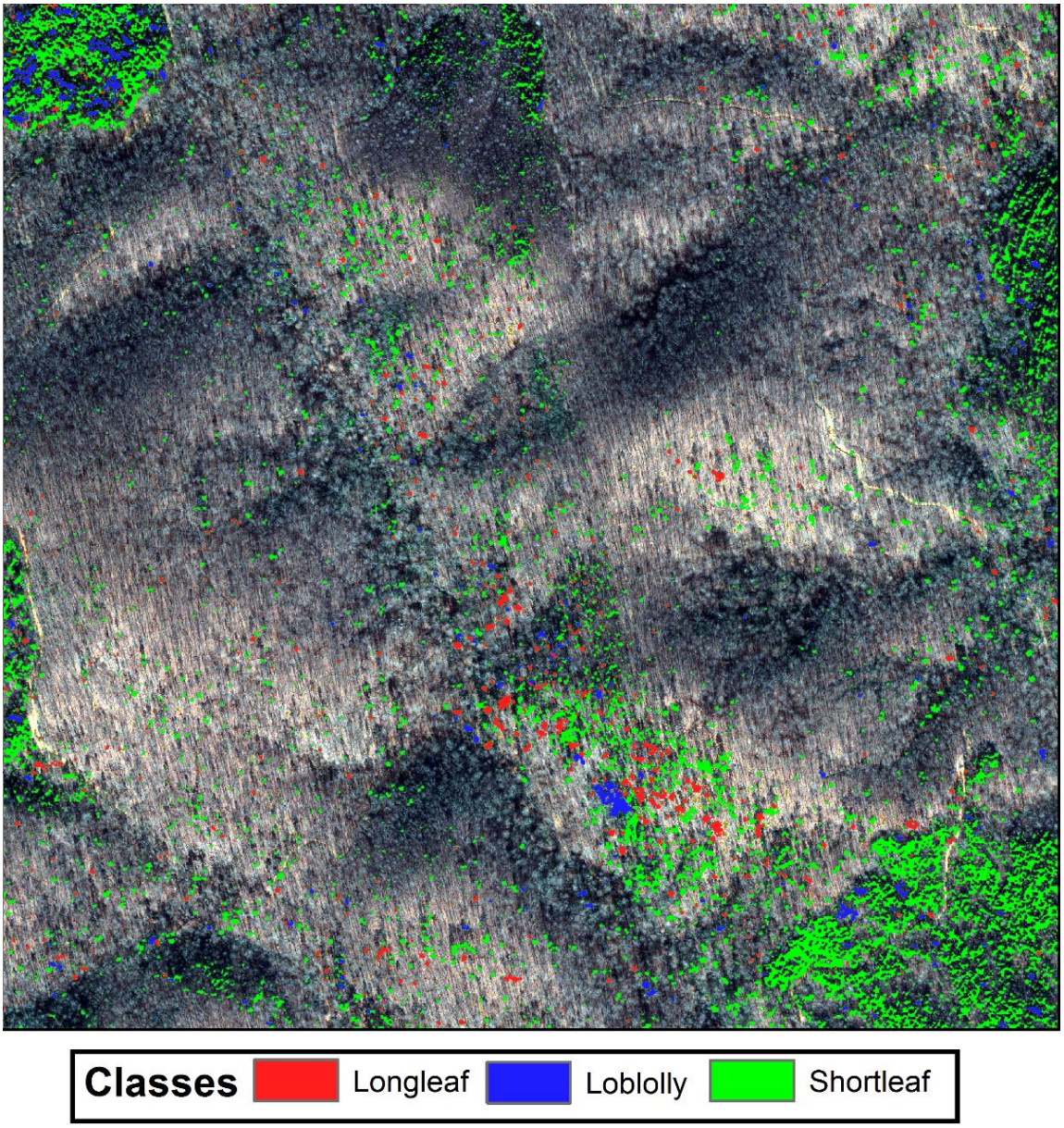

Figure 3.4. Distribution Of Classified Image Objects Throughout Fraley Grove In The UNF. Red Canopies Are Classified As Longleaf Pine, Blue Canopies Are Classified As Loblolly And Green Canopies Are Classified As Shortleaf.

Table 3.8. Individual Accuracy Results For Fraley Grove.

Overall Accuracy	(14564/16364) (Pixels)	89.00% (Percent)		
Kappa Coefficient	0.7802			
Pixels	**Shortleaf**	**Longleaf**	Total	
Shortleaf	7138	1164	8302	
Longleaf	636	7426	8062	
Total	7774	8590	16364	
Percent	**Shortleaf**	**Longleaf**	Total	
Shortleaf	91.82	13.55	50.73	
Longleaf	8.18	86.45	49.27	
Total	100	100	100	
	Commission	Omission	Commission	Omission
Class	(Percent)	(Percent)	(Pixels)	(Pixels)
Shortleaf	14.02	8.18	1164/8302	636/7774
Longleaf	7.89	13.55	636/8062	1164/8590
	Prod. Acc.	User Acc.	Prod. Acc.	User Acc.
Class	(Percent)	(Percent)	(Pixels)	(Pixels)
Shortleaf	91.82	85.98	7138/7774	7138/8302
Longleaf	86.45	92.11	7426/8584	7426/8062

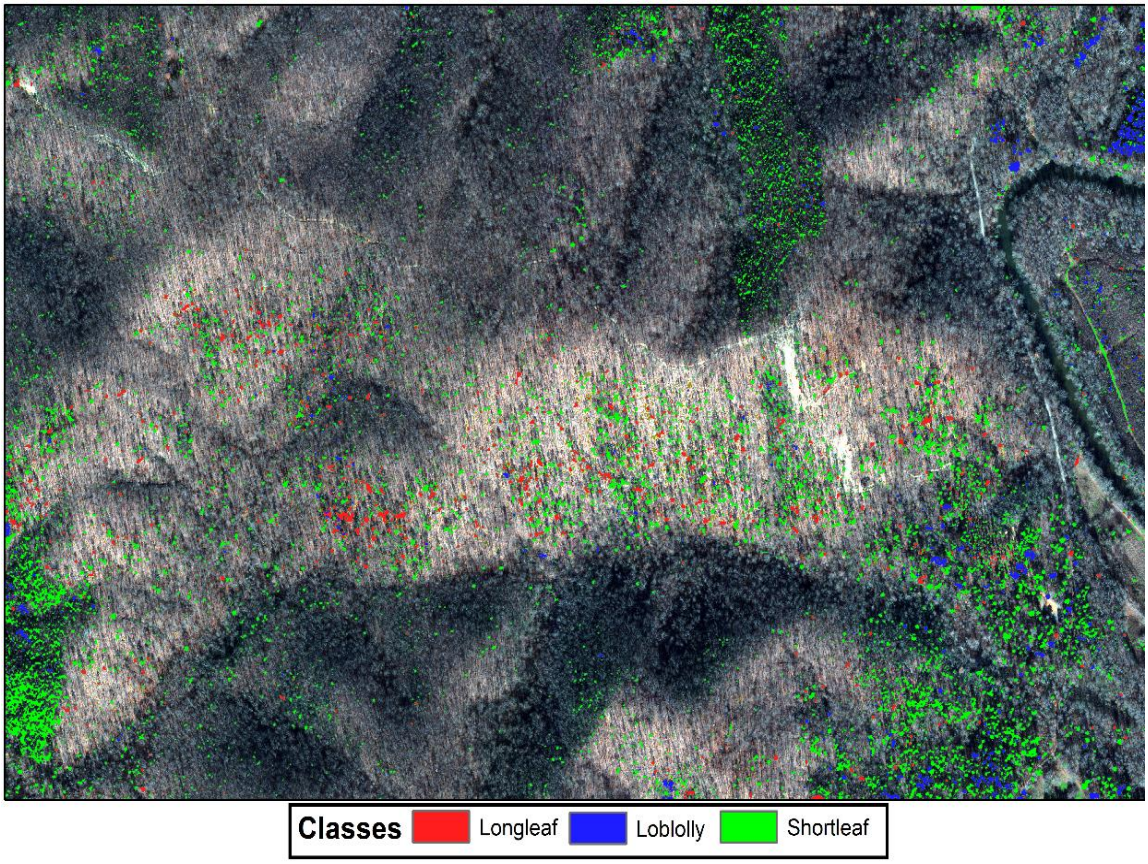

Figure 3.5. Distribution Of Classified Image Objects Throughout Goldmine Branch In The UNF. Red Canopies Are Classified As Longleaf Pine, Blue Canopies Are Classified As Loblolly And Green Canopies Are Classified As Shortleaf.

Table 3.9. Individual Accuracy Results For Goldmine Branch.

Overall Accuracy	**(24489/27575) (Pixels)**	**88.81% (Percent)**		
Kappa Coefficient	**0.8323**			
Pixels	**Shortleaf**	**Loblolly**	**Longleaf**	**Total**
Shortleaf	**8901**	**899**	**547**	**10347**
Longleaf	**0**	**1247**	**8281**	**9528**
Loblolly	**393**	**7307**	**0**	**7700**
Total	**9294**	**9453**	**8828**	**27575**
Percent	**Shortleaf**	**Loblolly**	**Longleaf**	**Total**
Shortleaf	**95.77**	**9.51**	**6.2**	**37.52**
Longleaf	**0**	**13.19**	**93.8**	**34.55**
Loblolly	**4.23**	**77.3**	**0**	**27.92**
	Commission	**Omission**	**Commission**	**Omission**
Class	**(Percent)**	**(Percent)**	**(Pixels)**	**(Pixels)**
Shortleaf	**13.98**	**4.23**	**1446/10347**	**393/9294**
Longleaf	**13.09**	**6.2**	**1247/9528**	**547/8828**
Loblolly	**5.1**	**22.7**	**393/7700**	**2146/9453**
	Prod. Acc.	**User Acc.**	**Prod. Acc.**	**User Acc.**
Class	**(Percent)**	**(Percent)**	**(Pixels)**	**(Pixels)**
Shortleaf	**95.77**	**86.02**	**8901/9294**	**8901/10347**
Longleaf	**93.8**	**86.91**	**8281/8828**	**8281/9528**
Loblolly	**77.3**	**94.9**	**7307/9453**	**7307/7700**

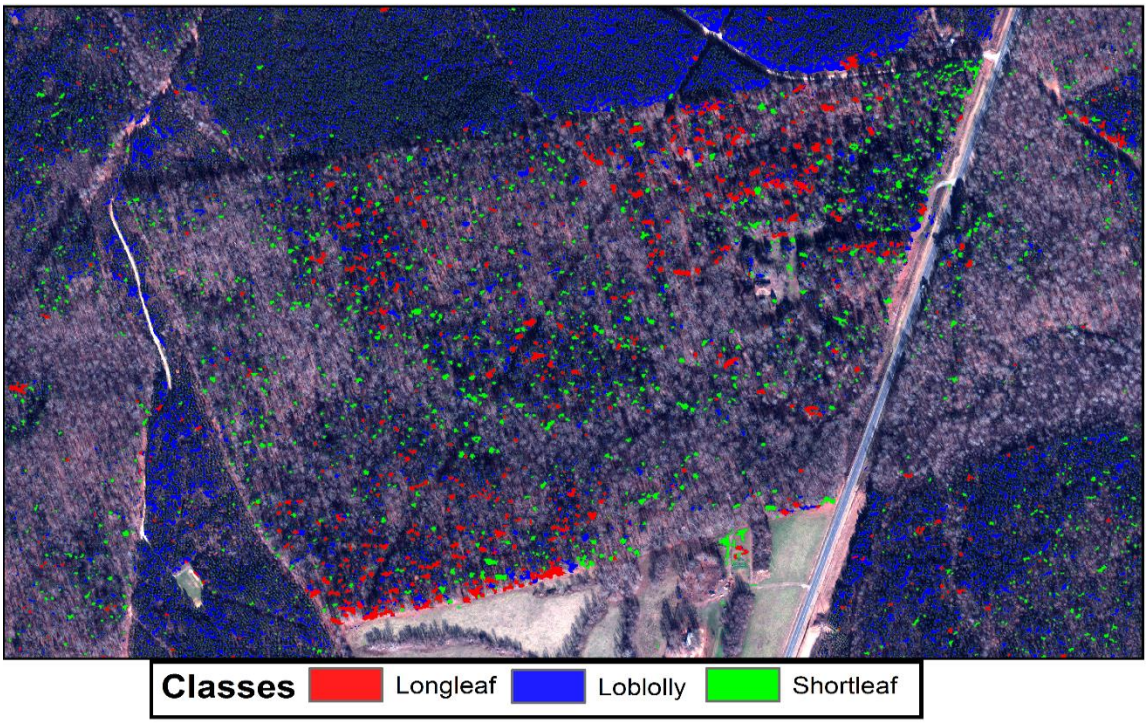

Figure 3.6. Distribution Of Classified Image Objects Throughout Nichols Tract In The UNF. Red Canopies Are Classified As Longleaf Pine, Blue Canopies Are Classified As Loblolly And Green Canopies Are Classified As Shortleaf.

Table 3.10. Individual Accuracy Results For Nichols Tract.

Overall Accuracy	**(33966/36702) (Pixels)**	**92.54% (Percent)**		
Kappa Coefficient	**0.8861**			
Pixels	**Shortleaf**	**Loblolly**	**Longleaf**	**Total**
Shortleaf	**257**	**8258**	**12**	**8527**
Longleaf	**10494**	**2045**	**418**	**12957**
Loblolly	**0**	**4**	**15214**	**15218**
Total	**9294**	**9453**	**8828**	**27575**
Percent	**Shortleaf**	**Loblolly**	**Longleaf**	**Total**
Shortleaf	**2.39**	**80.12**	**0.08**	**23.23**
Longleaf	**97.61**	**19.84**	**2.67**	**35.3**
Loblolly	**0**	**0.04**	**97.25**	**41.46**
	Commission	**Omission**	**Commission**	**Omission**
Class	**(Percent)**	**(Percent)**	**(Pixels)**	**(Pixels)**
Shortleaf	**3.15**	**19.88**	**269/8527**	**2049/10307**
Longleaf	**19.01**	**2.39**	**2463/12957**	**257/10751**
Loblolly	**0.03**	**2.75**	**4/15218**	**430/15644**
	Prod. Acc.	**User Acc.**	**Prod. Acc.**	**User Acc.**
Class	**(Percent)**	**(Percent)**	**(Pixels)**	**(Pixels)**
Shortleaf	**97.61**	**80.99**	**10494/10751**	**10494/12957**
Longleaf	**80.12**	**96.85**	**8258/10307**	**8258/8527**
Loblolly	**97.25**	**99.97**	**15214/15644**	**15214/15218**

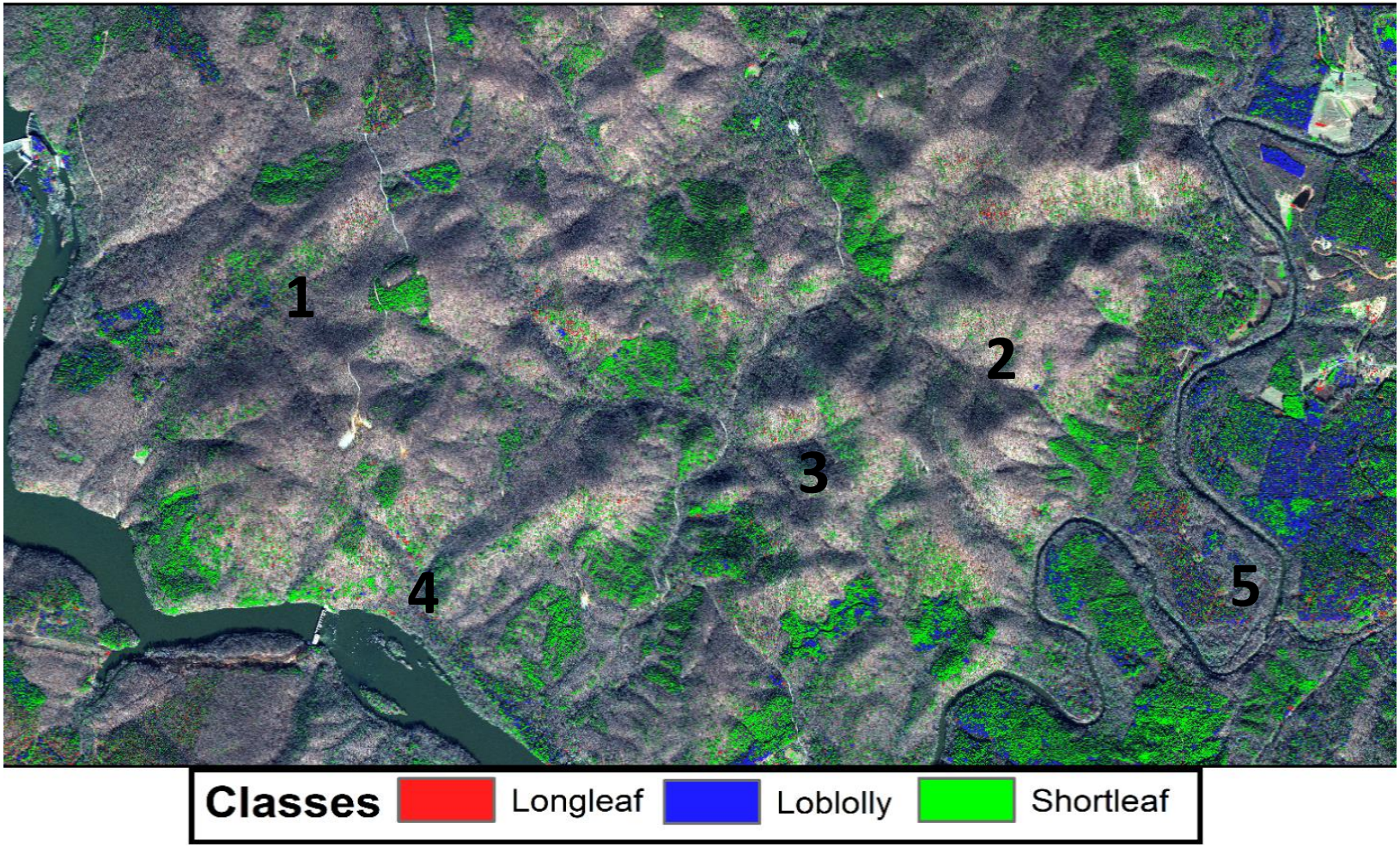

Figure 3.7. Distribution Of Classified Image Objects Throughout The Larger Portion Of The UNF. Red Canopies Are Classified As Longleaf Pine, Blue Canopies Are Classified As Loblolly And Green Canopies Are Classified As Shortleaf. Locations Of Ground Truth Investigation Numbered 1-5.

CHAPTER IV

DISCUSSION AND CONCLUSIONS

Through the spectral analysis of longleaf, shortleaf and loblolly pine growing in the UNF, a classification procedure has been developed that allows for the mapping of individual canopies within both montane and piedmont study areas. The overall accuracy for classifying longleaf pine were moderate, yet the implementation of this procedure over a larger area within the UNF resulted in high errors of omission and commission. This classification error could possibly be related to differences in spectral reflectance related to changes in elevation, slope, aspect and canopy height. At the individual-stand level, these influences are less pronounced, allowing for tree species to be accurately mapped with average OA = 90.11, and KS=0.83, but the spectral differences that can arise over larger areas with varying topography make it difficult to differentiate between the three species of pine present.

Previous studies have had success mapping longleaf pine with overall accuracies of 76% (Hughes et al. 1986), 85% (Van Aardt and Wynne 2007), 96% (Nieminen 2014), although the sites used in those did not contain areas with considerable topographic variation (> 100 m vertical relief) such as those found within the UNF. When comparing the overall accuracy of the species classification map produced for Nichols Tract (< 10 m vertical relief) to a similar study conducted by Nieminen (2014) in the De Soto National Forest in southeastern Mississippi, accuracy results are similar 92.54% ~96.00%. High

classification accuracy obtained for piedmont longleaf sampled from Nichols, and low accuracies for the montane sites suggest that topographic influences may be the major cause for reduced classification success in sites of high relief (> 100 m).

Spectral analysis of both montane and piedmont longleaf pine showed significant variation in reflectance values between the two varieties. This variance could be attributed to several of the influences examined in this study. Changes in slope and elevation appear to have significant influence on spectral reflectance across the electromagnetic range, and cause a decrease in reflectance with increases in topographic prominence. Additionally, tree canopy height is positively correlated with reflectance values for the longleaf sampled in this study. While reflectance increases with canopy height, canopy height tends to decrease with elevation and slope within the study areas, and this pattern is mirrored by decreases in canopy reflectance across all eight bands of the WorldView-2 imagery.

While determining the actual cause of reflectance variations due to topography and canopy height is beyond the scope of this research, it is possible that trees growing in areas of high topographic prominence may not have the same nutrient and water availability as those growing in areas of lower relief due to decreased soil depth on the rocky slopes. Additionally, environmental conditions in areas of higher elevation relating to precipitation and temperature gradients may reduce the trees' overall health, negatively influencing growth characteristics, resulting in shorter canopy heights, and subsequently decreasing reflectance for montane longleaf pine across the visible and near-infrared portions of the electromagnetic spectrum.

Incorporation of this measured spectral variance between the two classes of longleaf pine may allow future researchers to develop classification strategies capable of mapping longleaf even more accurately, permitting the discovery of unknown montane stands suitable for habitat restoration initiatives such as undergrowth thinning and prescribed burning.

Although ground verification of likely sites within the larger-classified area did not result in the location of new montane stands, the implementation of this procedure over other areas within the UNF may still produce favorable results for future studies. Montane communities of longleaf within North Carolina are rare, with only two known stands in existence: Fraley Grove and Goldmine Branch. While this research was not able to locate new montane stands within the study area, there is a possibility that no other stands present in the UNF. Implementation of this classification method in other adjacent land holdings within the National Forest is necessary to make this determination final.

To establish a methodology for returning the longleaf pine ecosystem to its historic extent across the southeastern United States, researchers must examine existing stands of these pines to determine certain parameters that provide optimum habitats for growth and subsequent regeneration. This process has been initiated by the National Forest Service and the Longleaf Alliance across the southeastern United States in delineated and protected stands (Jose et al., 2006). Research on the natural growth characteristics of longleaf pine has helped to reveal practices that positively influence the longevity of the species, including selective harvesting and prescribed fires in the

understory (Brockway, 2005). Locating new areas containing longleaf pine ecosystems, especially montane longleaf growing within areas of varying topography can allow for greater insight into their unique ecosystems.

Through the remote investigation of longleaf pine spectral properties from stands in the Uwharrie National Forest, a more detailed understanding of the spectral reflectance properties of the species has been has been developed for both montane and piedmont varieties. When attempting to generate species maps from remotely sensed data, a singular spectral signature derived reflectance data alone is insufficient to create accurate maps in areas of varying topography, tree age and height, as well as different seasons of imagery acquisition. Understanding how reflectance can vary between areas of differing elevation and slope is essential to mapping this species across large geographic areas like the Uwharrie National Forest.

REFERENCES

Aguilar, M. A., Saldaña, M. M., & Aguilar, F. J. (2013). GeoEye-1 and WorldView-2 pan-sharpened imagery for object-based classification in urban environments. *International Journal of Remote Sensing, 34*, 7, 2583-2606.

Asalhi A., H., andTeillet P. (2002). Transformed Difference Vegetation Index (TDVI) for Vegetation Cover Mapping. *In Proceedings of the Geoscience and Remote Sensing Symposium, IGARSS '02, IEEE International, Volume 5*

Blaschke, T., et al. (2008). Object-based image analysis: spatial concepts for knowledge-driven remote sensing applications. *Springer Science & Business Media*.

Brockway, D. G., United States, Forest Service, & Southern Research Station. (2005). *Restoration of longleaf pine ecosystems*. Asheville, NC: U.S. Dept. of Agriculture, Forest Service, Southern Research Station.

Carney, J. M. (2009). Use of multi-spectral imagery and LiDAR data to quantify compositional and structural characteristics of vegetation in red-cockaded woodpecker *(Picoides borealis)* habitat in North Carolina. Mississippi State: Mississippi State University.

Carter, G., et al. (1989). Effect of competition and leaf age on visible and infrared reflectance in pine foliage. *Plant, Cell & Environment 12*(3): 309-315.

Carter, G. A. (1993). Responses of Leaf Spectral Reflectance to Plant Stress. *American Journal of Botany 80*(3): 239-243.

Carter, G. A., Seal, M. R., & Haley, T. (1998). Airborne detection of southern pine beetle damage using key spectral bands. *Canadian Journal of Forest Research, 28*(7), 1040–1045.

Chen, Q., Vaglio Laurin, G., Battles, J. J., & Saah, D. (2012). Integration of airborne lidar and vegetation types derived from aerial photography for mapping aboveground live biomass. *Remote Sensing of Environment, 121*, 108–117.

Cipollini, M. L., Culberson, J., Strippelhoff, C., Baldvins, T., & Miller, K. (2012). Herbaceous Plants and Grasses in a Mountain Longleaf Pine Forest Undergoing Restoration: A Survey and Comparative Study. *Southeastern Naturalist, 11,* 4, 637-668.

Coops, N. C., et al. (2006). Assessment of QuickBird high spatial resolution imagery to detect red attack damage due to mountain pine beetle infestation. *Remote Sensing of Environment 103*(1): 67-80.

Di Vittorio, A. V., & Biging, G. S. (2009). Spectral identification of ozone-damaged pine needles. *International Journal of Remote Sensing*, *30*(12), 3041–3073.

Dowman, I., Jacobsen, K., & Konecny, G. (2014). *High Resolution Optical Satellite Imagery*. Dunbeath: Whittles Publishing.

Edelgard, C. M., Kush, J. S., & Meldahl, R. S. (2000). Vegetational Survey of a Montane Longleaf Pine Community at Fort McClellan, Alabama. *Castanea, 65,* 2, 147-154.

Ehlers, M., Gähler, M., & Janowsky, R. (January 01, 2003). Automated analysis of ultra-high resolution remote sensing data for biotope type mapping: new possibilities and challenges. *Isprs Journal of Photogrammetry and Remote Sensing, 57,* 5, 315-326.

Estornell, J., Ruiz, L. A., Velá zquez-Martí, B., & Hermosilla, T. (2012). Estimation of biomass and volume of shrub vegetation using LiDAR and spectral data in a Mediterranean environment. *Biomass and Bioenergy*, *46*, 710–721.

Gitelson, A., and M. Merzlyak. (1998) Remote Sensing of Chlorophyll Concentration in Higher Plant Leaves. *Advances in Space Research 22*: 689-692.

Goel, N., and W. Qin. (1994). Influences of Canopy Architecture on Relationships Between Various Vegetation Indices and LAI and Fpar: A Computer Simulation. *Remote Sensing Reviews 10* (1994): 309-347

Guo, C. F. and X. Y. Guo, Research on Typical Plant Spectral Distinguishable Characteristics by Mann-Whitney U-Test in Wild Duck Lake, *Advanced Materials Research*, Vol. 830, pp. 367-371, 2014

Haboudane, D., et al. (2004). Hyperspectral Vegetation Indices and Novel Algorithms for Predicting Green LAI of Crop Canopies: Modeling and Validation in the Context of Precision Agriculture. *Remote Sensing of Environment 90*: 337-352.

Holmgren, J., Persson, Å., & Söderman, U. (2008). Species identification of individual trees by combining high resolution LiDAR data with multi-spectral images. *International Journal of Remote Sensing*, *29*(5), 1537–1552.

Hughes, S. , J & L. Evans, D & Y. Burns, P. (1986). Identification of two pine species in high-resolution aerial MSS data. *Photogrammetric Engineering and Remote Sensing*, 56

James, F. C., Hess, C. A., Kicklighter, B. C., & Thum, R. A. (2001). Ecosystem Management and the Niche Gestalt of the Red-Cockaded Woodpecker in Longleaf Pine Forests. *Ecological Applications, 11*(3), 854–870.

Jensen, J. R. (2007). *Remote sensing of the environment: an earth resource perspective*. Upper Saddle River, NJ: Pearson Prentice Hall.

Jose, S., Jokela, E. J., & Miller, D. L. (2006). *The longleaf pine ecosystem ecology, silviculture, and restoration*. New York: Springer.

Manjunath, K. R., Kumar, A., Meenakshi, M., Renu, R., Uniyal, S. K., Singh, R. D., Ahuja, P. S., ... Panigrahy, S. (March 01, 2014). Developing Spectral Library of Major Plant Species of Western Himalayas Using Ground Observations. *Journal of the Indian Society of Remote Sensing, 42,* 1, 201-216.

Martin, M. E., et al. (1998). Determining Forest Species Composition Using High Spectral Resolution Remote Sensing Data. *Remote Sensing of Environment* 65(3): 249-254.

Nieminen, M. F., et al. (2014). "Spectral separability of longleaf and loblolly pines in high-resolution satellite data.

Oswalt, C. M., J. A. Cooper, D. G. Brockway, H. W. Brooks, J. L. Walker, K. F. Connor, S. N. Oswalt, and R. C. Conner. 2012. History and current condition of longleaf pine in the Southern United States. Gen. Tech. Rep. SRS–166. 51p. USDA Forest Service, Southeastern Forest Experimental Station, Asheville, NC.

Patterson, T. W. and P.A. Knapp. 2016a. Observations on a Rare Old-Growth Montane Longleaf Pine Forest in Central North Carolina. *Natural Areas Journal* 36:153–161.

Peet, R. K. 2006. Ecological Classification of Longleaf Pine Woodlands. *The Longleaf Pine Ecosystem: Ecology, Silviculture, and Restoration* (ed. by S. Jose, E. Jokela and D. Miller), pp. 51–93. New York, NY: Springer.

Pu, R., & Landry, S. (2012). A comparative analysis of high spatial resolution IKONOS and WorldView-2 imagery for mapping urban tree species. *Remote Sensing of Environment, 124*, 516-533.

Richardson, A. D. and G. P. Berlyn (2002). Spectral Reflectance and Photosynthetic Properties of Betula papyrifera (Betulaceae) Leaves along an Elevational Gradient on Mt.Mansfield, Vermont, USA. *American Journal of Botany 89*(1): 88-94.

Richardson, A. D., et al. (2001). Spectral reflectance of Picea rubens (Pinaceae) and Abies balsamea (Pinaceae) needles along an elevational gradient, Mt. Moosilauke, New Hampshire, USA. *American Journal of Botany 88*(4): 667-676.

Rouse, J., R. Haas, J. Schell, and D. Deering. (1973). Monitoring Vegetation Systems in the Great Plains with ERTS. *Third ERTS Symposium, NASA*: 309-317.

Shamsoddini, A., Trinder, J. C., & Turner, R. (January 01, 2013). Pine plantation structure mapping using WorldView-2 multispectral image. *International Journal of Remote Sensing, 34*, 11, 3986-4007.

Sims, D. A. and J. A. Gamon (2002). Relationships between leaf pigment content and spectral reflectance across a wide range of species, leaf structures and developmental stages. *Remote Sensing of Environment 81*(2): 337-354.

Sripada, R., et al. (2006). Aerial Color Infrared Photography for Determining Early In-season Nitrogen Requirements in Corn. *Agronomy Journal 98*: 968-977.

Stokes, T. A., Samuelson, L. J., Kush, J. S., Farris, M. G., & Gilbert, J. C. (2010). Structure and Diversity of Longleaf Pine (Pinus palustris Mill.) Forest Communities in the Mountain Longleaf National Wildlife Refuge, Northeastern Alabama. *Natural Areas Journal, 30*, 2, 211-225.

Tucker, C. (1979). Red and Photographic Infrared Linear Combinations for Monitoring Vegetation. *Remote Sensing of Environment* 8: 127–150

Van Aardt, J. and R. Wynne (2007). Examining pine spectral separability using hyperspectral data from an airborne sensor: An extension of field- based results. *International Journal of Remote Sensing* 28(2): 431-436.

Van Aardt, J. and Wynne, R. H. (2001). Spectral Separability among Six Southern Tree Species. *Photogrammetric Engineering and Remote Sensing, 67,* 1367-1376.

Waser, L., Küchler, M., Jütte, K., & Stampfer, T. (2014). Evaluating the Potential of WorldView-2 Data to Classify Tree Species and Different Levels of Ash Mortality. *Remote Sensing, 6,* 5, 4515-4545.

Xiao, Q., Ustin, S. L., & McPherson, E. G. (2004). Using AVIRIS data and multiple-masking techniques to map urban forest tree species. *International Journal of Remote Sensing, 25,* 24, 5637-5654.

Yang, Z., P. Willis, and R. Mueller. (2008). "Impact of Band-Ratio Enhanced AWIFS Image to Crop Classification Accuracy." *Proceedings of the Pecora 17 Remote Sensing Symposium* (2008), Denver, CO